Specific bone cells produce DLL4 to generate thymus-seeding progenitors from bone marrow

Specific bone cells produce DLL4 to generate thymus-seeding progenitors from bone marrow

Vionnie W.C. Yu,[1,2,3] Borja Saez,[1,2,3] Colleen Cook,[1,2,3] Sutada Lotinun,[4,5] Ana Pardo-Saganta,[1,2,9] Ying-Hua Wang,[1,2,3] Stefania Lymperi,[1,2,3] Francesca Ferraro,[1,2,3] Marc H.G.P. Raaijmakers,[6] Joy Y. Wu,[7] Lan Zhou,[8] Jayaraj Rajagopal,[1,2,9] Henry M. Kronenberg,[7] Roland Baron,[4,7] and David T. Scadden[1,2,3]

CORRESPONDENCE
David T. Scadden:
david_scadden@harvard.edu

[1]Center for Regenerative Medicine, Massachusetts General Hospital, Boston, MA 02215
[2]Harvard Stem Cell Institute, Cambridge, MA 02215
[3]Department of Stem Cell and Regenerative Biology, Harvard University, Cambridge, MA 02215
[4]Department of Oral Medicine, Infection and Immunity, Harvard School of Dental Medicine, Boston, MA 02215
[5]Department of Physiology and STAR on Craniofacial and Skeletal Disorders, Chulalongkorn University, Bangkok 10330, Thailand
[6]Department of Hematology and Erasmus Stem Cell Institute, Erasmus University Medical Center Cancer Institute, 3015 CE Rotterdam, Netherlands
[7]Endocrine Unit, Department of Medicine, Massachusetts General Hospital and Harvard Medical School, Boston, MA 02215
[8]Department of Pathology, Case Western Reserve University, Cleveland, OH 44106
[9]Departments of Internal Medicine and Pediatrics, Pulmonary and Critical Care Unit, Massachusetts General Hospital, Boston, MA 02215

Production of the cells that ultimately populate the thymus to generate α/β T cells has been controversial, and their molecular drivers remain undefined. Here, we report that specific deletion of bone-producing osteocalcin (Ocn)-expressing cells in vivo markedly reduces T-competent progenitors and thymus-homing receptor expression among bone marrow hematopoietic cells. Decreased intrathymic T cell precursors and decreased generation of mature T cells occurred despite normal thymic function. The Notch ligand DLL4 is abundantly expressed on bone marrow Ocn$^+$ cells, and selective depletion of DLL4 from these cells recapitulated the thymopoietic abnormality. These data indicate that specific mesenchymal cells in bone marrow provide key molecular drivers enforcing thymus-seeding progenitor generation and thereby directly link skeletal biology to the production of T cell–based adaptive immunity.

Abbreviations used: 7-AAD, 7-amino-actinomycin D; anti–hHB-EGF, anti–human heparin-binding EGF-like growth factor; CCL12, chemokine (C-C motif) ligand 12; CCR, C-C chemokine receptor type; CFDA-SE, carboxyfluorescein diacetate succinimidyl ester; CFU-Ob, colony forming unit-osteoblast; CLP, common lymphoid progenitor; CMP, common myeloid progenitor; CTX, C-terminal telopeptide of type I collagen; DAPT, *N*-[*N*-(3,5-difluorophenacetyl)-l-alanyl]-S-phenylglycine t-butyl ester; DLL, Delta-like ligand; DT, diphtheria toxin; DTR, DT receptor; G-CSF, granulocyte colony-stimulating factor; GMP, granulocyte and macrophage progenitor; GSEA, gene set enrichment analysis; GvHD, graft-versus-host disease; LKS, lineage^{Lo}c-Kit$^+$Sca$^+$; LKS SLAM, lineage^{Lo}c-kit$^+$Sca$^+$CD48$^-$ CD150$^+$; LT HSC, long-term hematopoietic stem cell; MEP, megakaryocyte erythroid progenitor; Mib1, Mindbomb1; MPP, multipotent progenitor; Mx1-Cre, B6.Cg-Tg(Mx1-Cre)1Cgn/J; NICD, notch intracellular domain; N.Oc/B.Pm, number of osteoclasts/bone perimeter; Ocn, osteocalcin; OcnCre-Topaz, C57BL/6-Tg(BGLAP-Topaz)1Rowe/J Osx Osterix; P1NP, N-terminal propeptide of type I procollagen; poly(I:C), polyinosinic:polycytidylic acid; Pofut1, protein O-fucosyltransferase 1; PSGL1, P-selectin goycoprotein ligand-1; PTH, parathyroid hormone; SJL, B6.SJL-*Ptprc*^{a}*Pepc*^{b}/BoyJ; ST HSC, short-term hematopoietic stem cell; TRAP, tartrate-resistant acid phosphatase.

Bone mesenchymal cells are central participants in hematopoiesis, providing niches regulating stem and progenitor cells. Lymphopoiesis depends on tissues outside the bone marrow for terminal maturation, but antigen-independent specification of lymphoid lineages is hypothesized to occur in bone marrow. B cell generation has been definitively shown to involve osteolineage cells, whereas T cell generation remains controversial (Visnjic et al., 2004; Zhu et al., 2007; Wu et al., 2008). Deletion of CXCL12 in early osteolineage cells decreased B cell progenitors, whereas deletion of osteocytes produced dramatic metabolic changes, primary damage to thymus, and decreased B and T cell generation through an undefined molecular mechanism (Ding and Morrison, 2013; Greenbaum et al., 2013; Sato et al., 2013). Co-culture of hematopoietic progenitors with bone marrow stroma cells overexpressing Notch ligands enabled T cell lineage generation in vitro (Holmes and Zúñiga-Pflücker, 2009), but whether this recapitulates in vivo events in the bone marrow microenvironment is unclear (Uhmann et al., 2011).

The details of the prethymic process are of increasing interest given that early thymic progenitors may serve as a limiting substrate in immune reconstitution after transplant (Zlotoff et al., 2011). It has been shown that providing

The Rockefeller University Press $30.00
J. Exp. Med. 2015 Vol. 212 No. 5 759–774
www.jem.org/cgi/doi/10.1084/jem.20141843

The Journal of Experimental Medicine

ex vivo generated human pro–T cells improved T cell reconstitution, thymic architecture, and immunological competence in immunodeficient mice (Zakrzewski et al., 2006; Awong et al., 2013). Therefore, understanding and modulating the production of bone marrow–derived cells that can populate the thymus may have practical consequences in medicine.

RESULTS

We generated mouse strains in which Cre recombinase produced by either the *Osteocalcin* promoter expressed in mature osteoblasts and osteocytes, or the *Osterix* promoter expressed in distinct, more immature subsets of bone cells, drives expression of the diphtheria toxin (DT) receptor (DTR) on cell surface ($OcnCre^{+/-}$;iDTR and $OsxCre^{+/-}$;iDTR, respectively; $OcnCre^{+/-}$ and $OsxCre^{+/-}$ served as controls). Specific in vivo cell ablation was achieved by intraperitoneal injection of DT. Daily injections into both control and mutant animals began at age 4 wk, and by 6 wk a difference in body size was noted in both the $OsxCre^{+/-}$;iDTR and $OcnCre^{+/-}$;iDTR mutant mice compared with littermate controls, which is consistent with inhibition of bone formation (Fig. 1 A). In early experiments, $OsxCre^{+/-}$;iDTR and $OcnCre^{+/-}$;iDTR animals without DT treatment were assessed and no phenotypic difference with the $OsxCre^{+/-}$ and $OcnCre^{+/-}$ controls were noted and therefore are not presented further. The T lymphopenic effect was observed only in the $OcnCre^{+/-}$;iDTR strain and not the $OsxCre^{+/-}$;iDTR strain, and thus it is the focus of this work.

Histomorphometry revealed ∼70% deletion of osteoblasts and osteocytes in the $OcnCre^{+/-}$;iDTR mutants (Fig. 1, B and C). To evaluate whether DTR was expressed in the correct cells in bone marrow, immunohistochemistry for DTR without toxin injection was performed and demonstrated overlap with anti-Ocn staining (Fig. 1 D). TUNEL staining after DT administration demonstrated overlap with osteocalcin-specific antibodies (Fig. 1 E), indicating selective cell killing.

Osteoclasts were assessed by TRAP staining and histomorphometry (Fig. 1 F), and measuring endogenous osteoclast activity (Fig. 1 G); these indices were not affected by 2 wk of toxin administration in $OcnCre^{+/-}$;iDTR mice. Testing whether osteolineage cell depletion might lead to an excess of primitive responding bone progenitor cells, primitive mesenchymal progenitors were assessed by colony forming unit-osteoblast (CFU-Ob) assays and found to be unchanged (Fig. 1 H). No detectable changes in $CD31^{-}CD45^{-}Ter119^{-}LepR^{+}$ stromal cells were observed (Fig. 1 I).

Despite the changes in bone morphology, overall bone marrow cellularity was unaffected as were blood and bone marrow counts of mature hematopoietic cells except lymphoid cells (Fig. 2 A). This was associated with reduced common lymphoid progenitors (CLPs) within the bone marrow and blood and in particular, CLP with T cell potential ($Lineage^{-}Sca^{+}cKit^{+}IL7R^{+}Thy1.2^{-}Ly6D^{-}$; Inlay et al., 2009; Mansson et al., 2010; Fig. 2, B and C), whereas B-lineage biased CLP ($Lineage^{-}Sca^{+}cKit^{+}IL7R^{+}Thy1.2^{-}Ly6D^{+}$; Tsapogas et al., 2011; Welinder et al., 2011) and progenitors of other lineages, including common myeloid progenitor (CMP), granulocyte and macrophage progenitor (GMP), and megakaryocyte erythroid progenitor (MEP), were not changed (Fig. 2 B). We observed a decrease in bone marrow pro–B subsets, but not in prepro–B cells or downstream pre–B and mature B cells (Fig. 2 D). Spleen weight, cellularity, and B cell count were also not significantly affected. The decrease in B cell intermediates, whereas $Ly6D^{+}CLP$ were normal suggests that specification of B-lineage was not perturbed, but that support of downstream differentiation events was abnormal, as has been seen in other osteolineage modifications (Zhu et al., 2007; Wu et al., 2008; Ding and Morrison, 2013; Greenbaum et al., 2013).

Accompanying the decreased T-competent CLPs in the bone marrow, downstream T-progenitor and mature cells in the thymus were also reduced (Fig. 2 E). We confirmed that $Ly6D^{-}CLP$ are T cell competent by transplantation (Fig. 3 A), and we examined populations others have used in defining T-competent CLP ($Flt3^{+}Ly6D^{-}CLP$ [Karsunky et al., 2008; Inlay et al., 2009] and CLP-1 [Scimone et al., 2006; Krueger and von Boehmer, 2007]). Decreases in each of these was seen with Ocn^{+} cell depletion and levels were comparable to $Ly6D^{-}CLP$ (unpublished data). Of note, there was no detectable DTR expressed on CLPs to suggest ectopic cell killing by DT.

Despite the increased immunophenotypic hematopoietic stem and progenitor cell (HSPC; $Lin^{-}Sca^{+}cKit^{+}CD48^{-}CD150^{+}$) number, cell cycling (Fig. 3, B–D), and increased reconstitution at 8 and 12 wk after bone marrow transplantation (Fig. 3 E), no long-term advantage in reconstitution was scored at 16 wk after primary transplantation in a competitive transplant assay. There was also no detectable change in secondary transplantation of cells from the Ocn^{+} deleted animals. These data are consistent with altered cycling of long-term HSC (LT HSC) without an effect on the functionally defined reconstituting ability of these cells by primary and secondary transplantation. The data indicate an effect on short-term HSC (ST HSC) and do not exclude an effect on LT HSC, just not a change in their reconstituting ability from the Ocn^{+} cell depleted bone marrow. It is possible that longer term exposure to the Ocn^{+} cell–depleted marrow would affect functional LT HSC number. It is also possible that other important functional changes were induced, but not measured in our studies.

To evaluate the microenvironment dependence of T-lymphopoiesis, WT congenic hematopoietic cells were transplanted into $OcnCre^{+/-}$;iDTR hosts; the abnormal lymphopoietic phenotype was recapitulated (Fig. 4 A). Reciprocally, $OcnCre^{+/-}$;iDTR mutant donor bone marrow reverted to normal phenotype when transplanted into WT congenic hosts (Fig. 4 B). Testing whether the effect was on the basis of differential cell proliferation or survival, CLP cell cycling by Ki67 and DAPI staining and cell death by Annexin V and 7-amino-actinomycin D (7-AAD) staining were assessed and no significant differences were observed (Fig. 4 C), suggesting alternative mechanisms must be active.

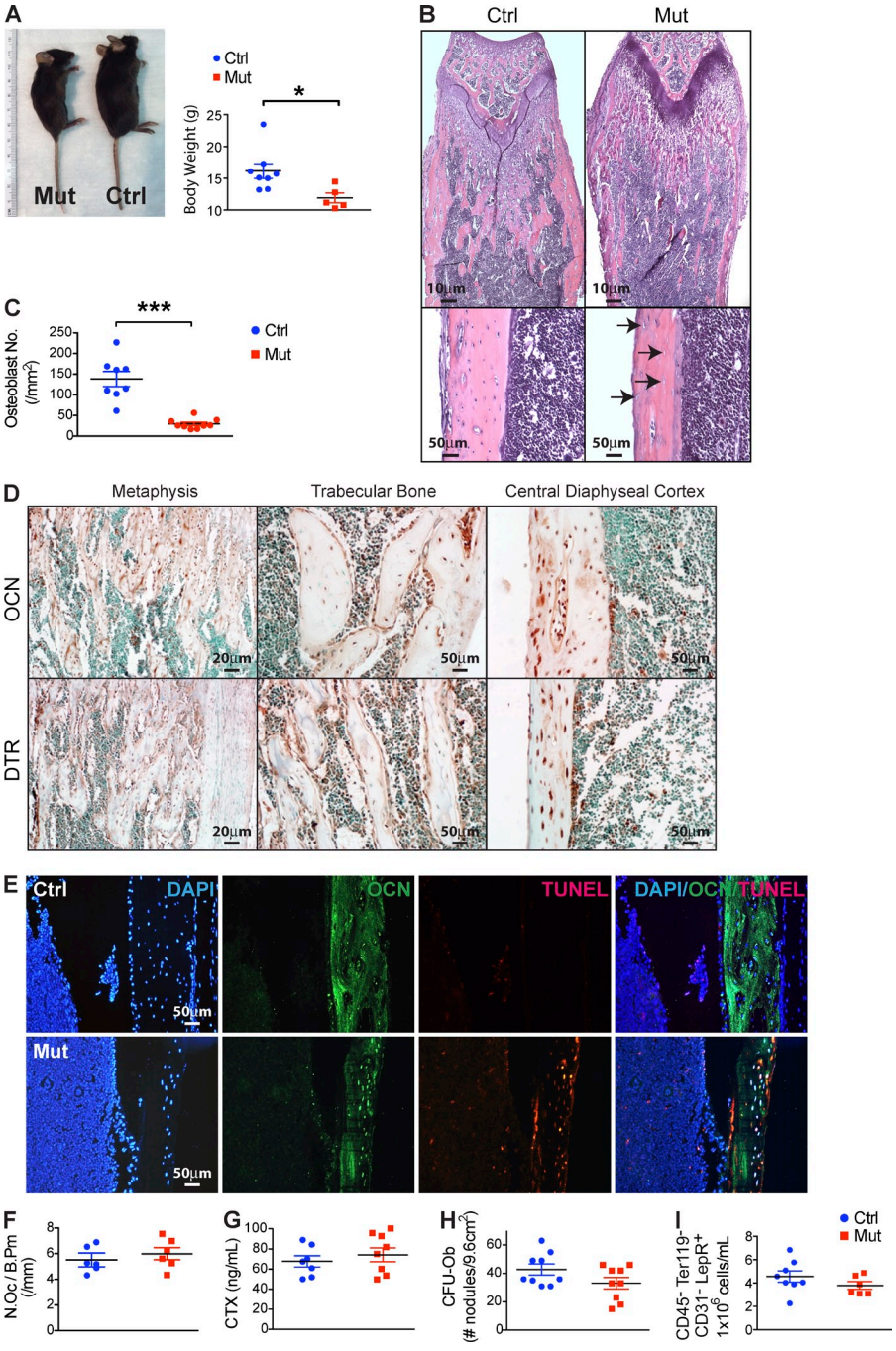

Figure 1. Ocn⁺ cell–specific deletion in vivo without altering osteoclastogenesis and mesenchymal progenitors. (A) WT mice (Ctrl) Ocn⁺ osteolineage cell deletion mice (Mut) were monitored for body size and weight; $n = 8$–10 mice/group. Data show mean ± SEM. (B) Femurs and tibiae in the OcnCre$^{+/-}$;iDTR mutants or WT (Ctrl) mice were assessed histologically. Bottom images are at a higher magnification with arrows pointing to empty lacunae within the cortex and altered endosteal surface; images reflect comparable findings in all animals; $n = 8$/experiment. (C) Osteoblasts in the OcnCre$^{+/-}$;iDTR and WT mice were quantitated by histomorphometry; $n = 7$–8 mice/group. Data show mean ± SEM. (D and E) Ocn and DTR expression was examined in bone sections from untreated OcnCre$^{+/-}$;iDTR by immunohistochemistry using Ocn- and DTR-specific antibodies (D), or by immunofluorescence using Ocn-specific antibodies and TUNEL staining after DT treatment (E); $n = 6$ mice/group. (F) Osteoclast numbers were assessed by TRAP staining ($n = 6$ mice/group) and (G) osteoclast activity by collagen breakdown in sera using ELISA assay; $n = 7$–8 mice/group. Data show mean ± SEM. (H) Mesenchymal progenitor activity in the bone marrow of OcnCre$^{+/-}$;iDTR mutants or WT controls was assessed by CFU-Ob assay; $n = 9$ mice/group. Data show mean ± SEM. (I) CD31$^-$CD45$^-$Ter119$^-$LepR$^+$ cells in the bone marrow stroma of OcnCre$^{+/-}$;iDTR mutants and controls were quantified by flow cytometry; $n = 6$–7 mice/group. Data show mean ± SEM. (A–I) For each experiment, 3–6 independent repeats were performed.

Since Notch is an essential determinant of T-lymphoid commitment and is required for progression through the DN stage (Sambandam et al., 2005; Tan et al., 2005; Visan et al., 2006; Rothenberg et al., 2010; Love and Bhandoola, 2011), we hypothesized that Notch may be participating in the phenotype observed. Notch participation in T-lymphopoiesis before thymic location was previously discounted (Krueger and von Boehmer, 2007), but the cells that were examined have since been shown to be precursors of extrathymic maturation and do not represent thymic progenitors (Luche et al., 2013). In contrast, some studies have reported Notch signaling in bone marrow T cell progenitors (Harman et al., 2005; Maeda et al., 2007). We assessed bone marrow CLP by flow cytometry for evidence of activated, or cleaved Notch and lower levels were observed in OcnCre$^{+/-}$;iDTR mutants (Fig. 5 A). This was validated by a decrease in several Notch target genes by qPCR (Fig. 5 B). The five mammalian Notch ligands, Jagged1, Jagged2, Delta-like 1 (DLL1), DLL3, and DLL4 were evaluated by qPCR and DLL4 was selectively decreased in bones from OcnCre$^{+/-}$;iDTR mutant mice (Fig. 5 C). Using a OsxCre-mCherry;OcnCre-Topaz double transgenic mouse model, we selectively labeled Osx$^+$ cells red, Ocn$^+$ cells green,

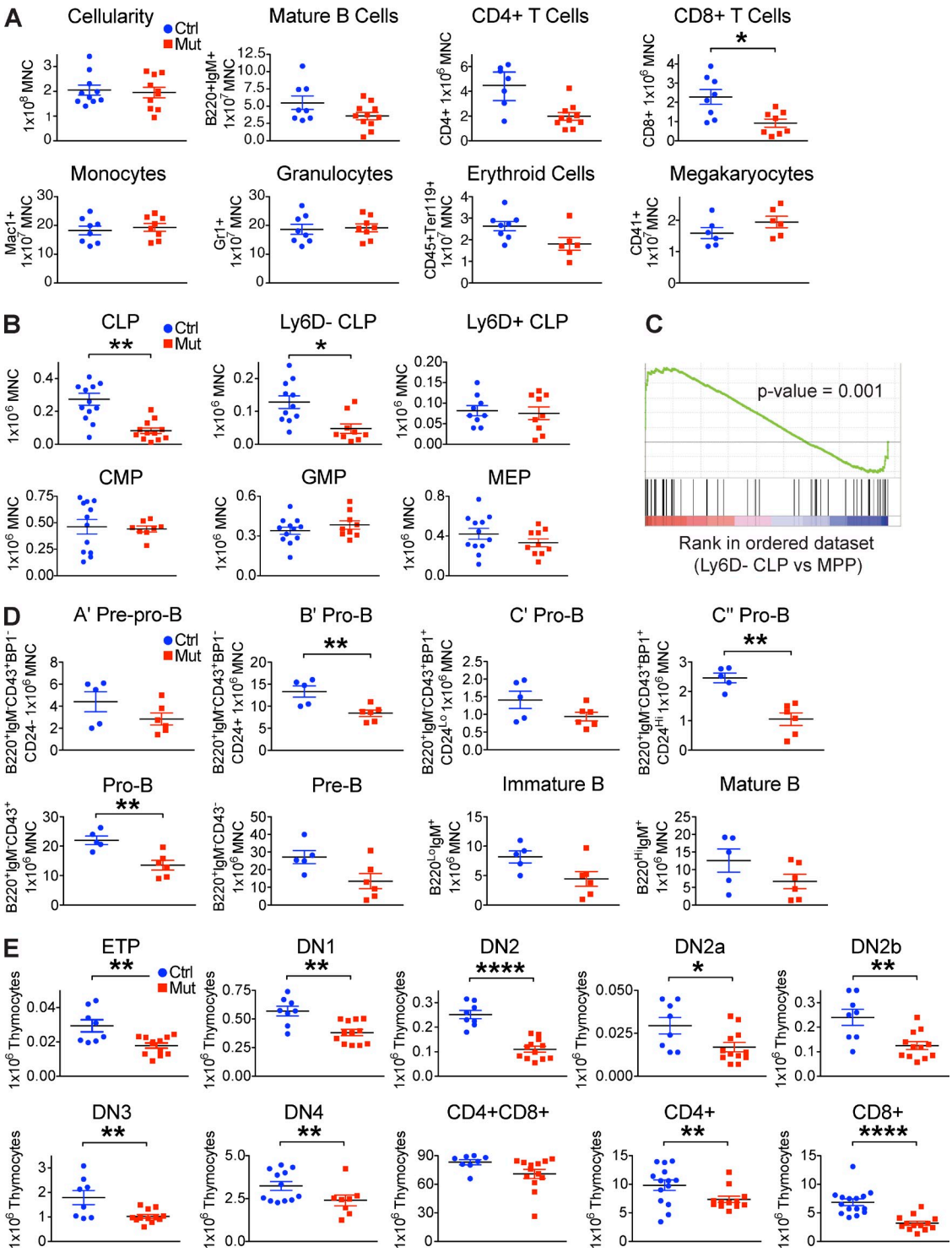

Figure 2. Ocn⁺ cell deletion decreases T cell competent lymphoid progenitors and T lineage cells. (A) Flow cytometric evaluation of lymphoid, myeloid, erythroid, and megakaryocytic mature cells and (B) T cell competent (Ly6D⁻) CLP, B potential enriched (Ly6D⁺) CLP, CMP, GMP, and MEP populations in the bone marrow of control and Ocn⁺ cell–deleted animals. Minimum of three independent experiments; n = 8–16 mice/group. Data show mean ± SEM. (C) Gene set enrichment analysis (GSEA) comparing Ly6D⁻ CLP versus multipotent progenitor (MPP) microarray data. Experiment was performed twice independently; n = 3/experiment. (D) Flow cytometric quantification of different stages of B progenitors and mature cells in the bone marrow of OcnCre;iDTR mutant and control littermates. Experiment was performed twice independently; n = 5–6 mice/group. Data show mean ± SEM. (E) Flow cytometric quantification of T cell subsets in the thymus. Minimum of four independent experiments; n = 8–12 mice/group. Data show mean ± SEM.

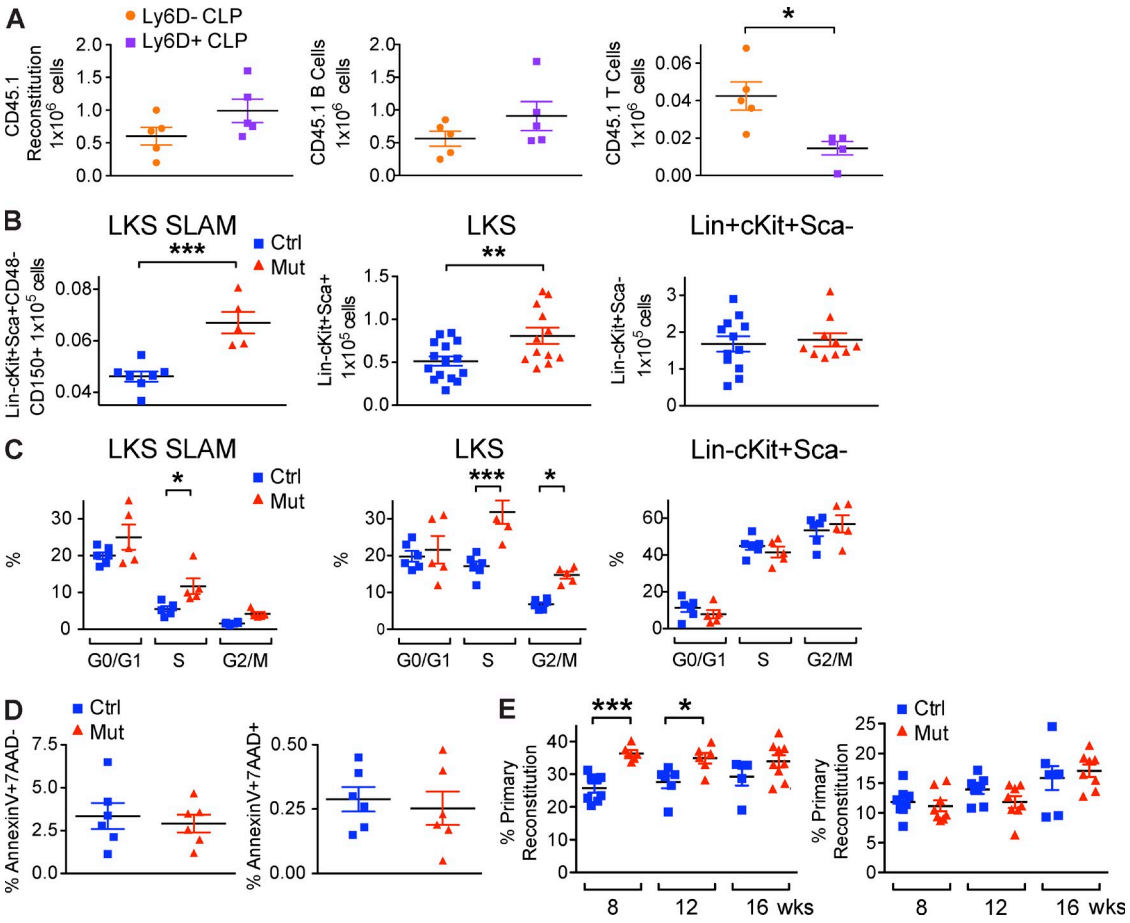

Figure 3. Lymphopenic phenotype in OcnCre;iDTR mice was not caused by a stem cell defect. (A) 44,000 flow sorted Ly6D$^-$ or Ly6D$^+$ CLPs from SJL (CD45.1) mice were intravenously transplanted into each of 10 nonirradiated C57BL/6J (CD45.2) recipients. Recipients were bled 3 wk after transplant for enumeration of donor-derived B and T reconstitution by staining with CD45.1, B220, CD4 and CD8 antibodies and analysis by flow cytometry. Experiment was performed twice independently; n = 10/experiment. Data show mean ± SEM. (B) Mature osteolineage cells were deleted from OcnCre;iDTR mice and hematopoietic stem cells (LKS SLAM), Lineage^{Lo}c-Kit$^+$Sca$^+$ (LKS) multipotent progenitors, and Lineage^{Lo}c-Kit$^+$Sca$^-$ cells were enumerated by flow cytometry. (C) Cell cycle analysis of the indicated cell populations was performed by flow cytometry. (D) Frequency of apoptotic (AnnexinV$^+$7-AAD$^-$) and necrotic (AnnexinV$^+$7-AAD$^+$) LKS SLAM, LKS, and Lineage^{Lo}c-Kit$^+$Sca$^-$ cells was assessed. Experiments were repeated 3 times independently; n = 5–16 mice/group. Data show mean ± SEM. (E) CD45.2 OcnCre;iDTR mutant or control donor cells were mixed with CD45.1 SJL donor cells in a 1:1 ratio, injected into primary SJL recipients. Reconstitution was assessed at 8, 12, and 16 wk after transplantation. Bone marrow cells from primary recipients were harvested and transplanted into secondary recipients. Reconstitution was assessed at 8, 12, and 16 wk following transplantation. Transplantation was performed twice independently; n = 20–22 mice/experiment. Data show mean ± SEM.

and Osx$^+$Ocn$^+$ cells yellow. This system allowed clear distinction and isolation of different osteolineage subsets within the same animal by flow cytometry. Immunohistochemistry (Fig. 5 D) and gene expression data (Fig. 5 E) showed that Ocn$^+$ mature osteoblasts, but not other osteolineage cells, potently expressed DLL4, and both mRNA and protein were markedly reduced in OcnCre$^{+/-}$;iDTR mice with protein notably decreased at the endosteal interface. This change in DLL4 was associated with corresponding alterations in Notch target genes in CLPs in the bone marrow by gene set enrichment analysis (GSEA; Fig. 5, F and G). These data suggest that reduced DLL4 expression from Ocn$^+$ cells led to reduced intracellular Notch activation in the hematopoietic precursors within the bone marrow, thereby limiting T-lineage specification.

We tested whether Notch ligand expression specifically by Ocn$^+$ cells caused the lymphopoietic phenotype using the conditional OcnCreER;DLL4$^{Fl/Fl}$ strain. Ocn$^+$ cell-specific *DLL4* deletion resulted in significantly reduced Notch-activated CLP, T cell–competent Ly6D$^-$-CLP, and CCR7-expressing Ly6D$^-$-CLP (Fig. 6 A, discussed in the following paragraphs), with a decrease comparable in magnitude to that seen with Ocn$^+$ cell depletion (Fig. 2 B). Thymic intermediates and blood T-lymphocytes were also decreased (Fig. 6 A).

Similar changes were noted when *Mindbomb1* (*Mib1*) encoding an E3-ligase necessary for Notch ligand processing (Koo et al., 2005), was deleted in Ocn$^+$ cells (Fig. 6 B). Together, these data demonstrate the role of Notch ligands expressed by Ocn$^+$ cells as the basis for the decrease in T-lymphopoiesis.

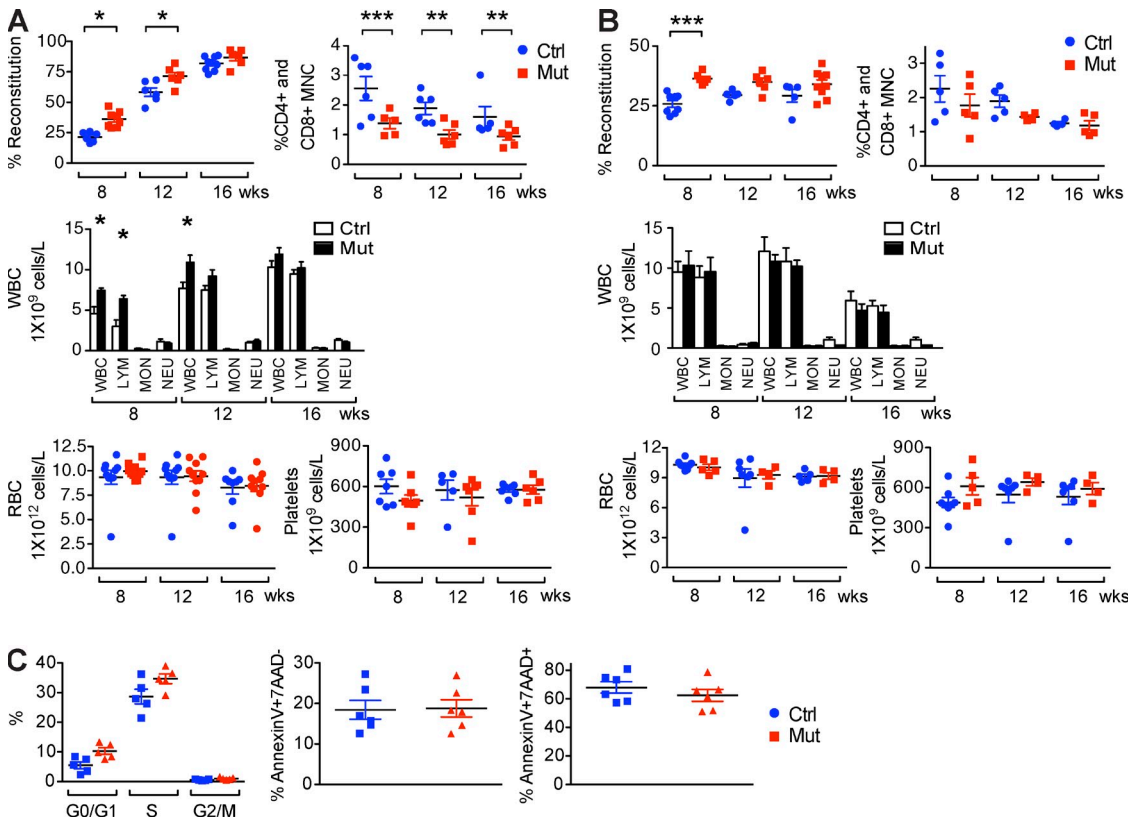

Figure 4. Ocn⁺ cell regulation of T lymphopoiesis is dependent on bone marrow microenvironment. (A) 10^6 WT CD45.1 hematopoietic bone marrow cells were transplanted into lethally irradiated CD45.1 OcnCre;iDTR hosts that were untreated or treated with DT. Animals were bled at 8, 12, and 16 wk after transplantation for blood count and assessment of hematopoietic reconstitution by flow cytometry. (B) 5×10^5 bone marrow cells from either control or mutant CD45.2 OcnCre$^{+/-}$;iDTR donors were mixed with 5×10^5 CD45.1 SJL bone marrow competitors in a 1:1 ratio and transplanted into lethally irradiated WT SJL recipients. Animals were bled at 8, 12, and 16 wk after transplantation for blood count and hematopoietic reconstitution by flow cytometry. (A and B) Two independent transplantations were performed; $n = 20–22$ mice/experiment. Data show mean ± SEM. (C) Cell cycle status, apoptosis, and necrosis in CLPs in OcnCre$^{+/-}$;iDTR mutants and controls were assessed by flow cytometry. 2 independent experiments; $n = 5–6$ mice/group. Data show mean ± SEM.

Testing of Notch-signaling in hematopoietic cells was then performed by several models. The *Protein O-fucosyltransferase1* gene product (Pofut1) transfers O-fucose to the EGF-like repeats on Notch and is required for the binding of Delta-like ligands (Yao et al., 2011). Deleting it using Mx1-Cre$^{+/-}$;Pofut1$^{Fl/Fl}$ mice revealed decreased CLP and Ly6D$^-$-CLP compared with controls (Fig. 7 A). Because Pofut1 does not act exclusively on Notch receptors, the downstream signaling mediator RBP-Jκ was also assessed. Mx1-Cre deletion of RBP-Jκ compromised bone marrow CLP and Ly6D$^-$-CLP (Fig. 7 B). Further, intrafemoral injection of the γ-secretase inhibitor *N*-[*N*-(3,5-difluorophenacetyl)-l-alanyl]-S-phenylglycine t-butyl ester (DAPT) reduced CLP and Ly6D$^-$-CLP on the ipsilateral side (Fig. 8 A). Lastly, intravenously transplanted 10^6 Lin$^-$ hematopoietic progenitor cells from Mx1Cre;LSL-NICD-GFP mice expressing a dominant-active Notch intracellular domain (NICD) rescued the OcnCre;iDTR lymphoid defect in Ly6D$^-$-CLP and Ly6D$^-$CCR7$^+$-CLP compared with Mx1Cre;LSL-GFP controls (Fig. 8 B). Collectively, these in vivo genetic mouse models confirm the role of Notch signaling in early T-lineage differentiation: altering bone marrow generation of thymic progenitors. Further, the comparable changes seen when either the ligand or receptor were modified suggest that the interaction of Ocn$^+$ cell and hematopoietic cells may be direct rather than through other microenvironmental cell types and argue against the phenotype being on the basis of stress or secondary metabolic changes.

The abnormality in T-lymphopoiesis could reflect dysfunction of the thymus itself or of the immigrants to the thymus arriving from the bone marrow. To assess this, we evaluated osteocalcin and DTR expression in thymic tissue, but found none by immunohistochemistry; no change in thymic histology or thymic DLL4 mRNA by quantitative PCR was observed after Ocn$^+$ cell depletion (unpublished data). To determine if thymic function was altered in Ocn$^+$ cell–deleted animals, we adoptively transferred WT Ly6D$^-$-CLP or Lin$^-$Sca$^+$cKit$^+$Flt3$^+$ hematopoietic progenitor cells into the thymi of either OcnCre$^{+/-}$;iDTR mutant or control recipients in vivo, and detected no difference in thymocyte maturation.

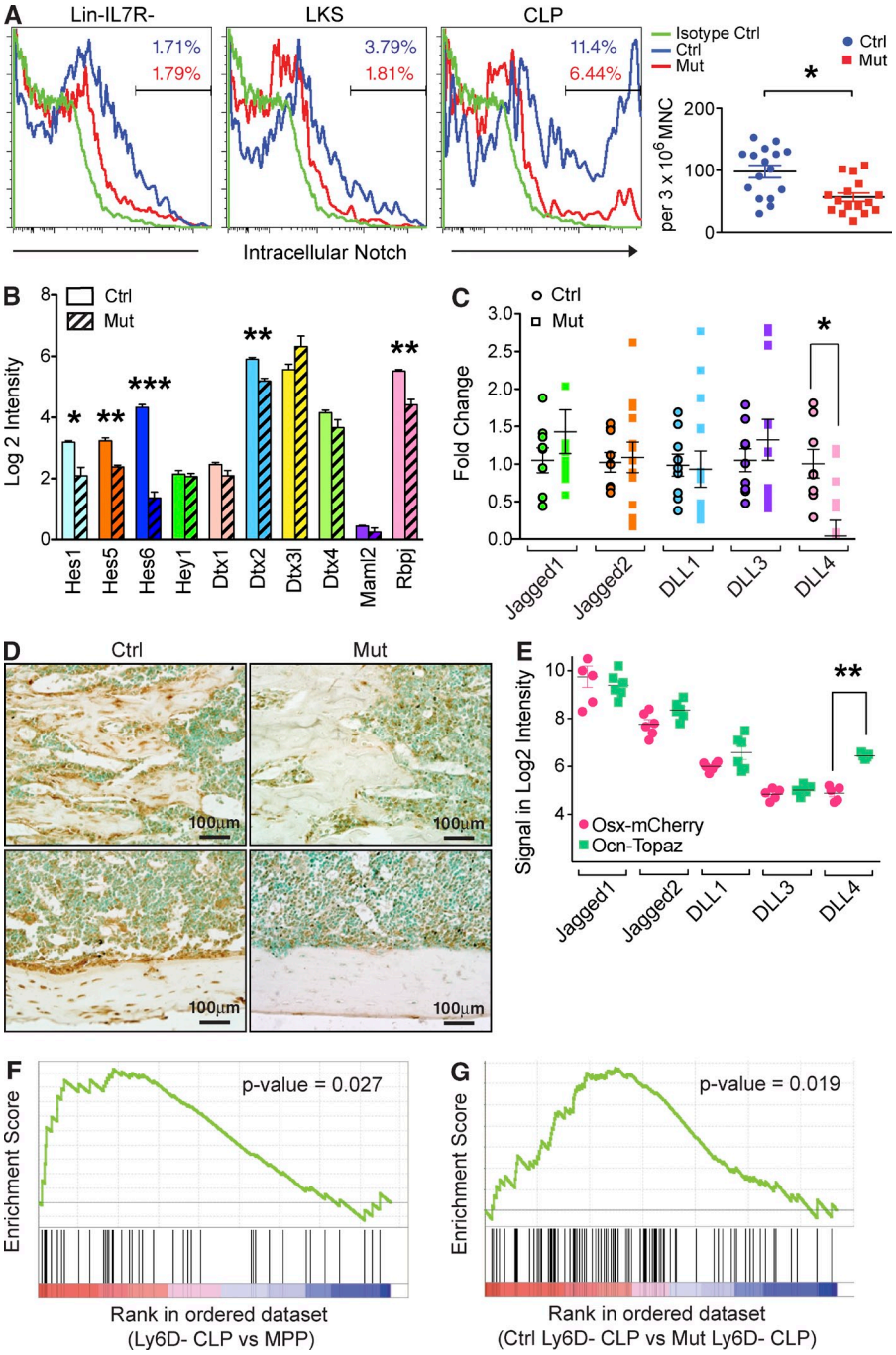

Figure 5. Reduced DLL4 in the bone marrow of Ocn⁺ cell depleted mice led to decreased Notch signaling in CLP. (A) Intracellular Notch signaling was assessed by flow cytometry in the indicated cell populations. Representative flow plots are shown, and data are summarized by dot plot (right). Three independent experiments; n = 16–17 mice/group. Data show mean ± SEM. (B) Expression of the indicated Notch target genes in Ly6D⁻ CLP from OcnCre$^{+/-}$;iDTR mutants and controls. Mutant and WT mice were treated with DT for 28 d before being subjected to flow cytometry for Ly6D⁻ CLP isolation and quantitative PCR. Two independent experiments; n = 12 mice/group. Data show mean ± SEM. (C) Expression of the Notch ligands in the bones of OcnCre$^{+/-}$;iDTR DT-treated and control animals was assessed by qPCR. Mice were examined after 28 d after DT treatment. Three independent experiments; n = 12–14 mice/group. Data show mean ± SEM. (D) DLL4 expression in bone sections from control or Ocn⁺ cell deleted animals was assessed by immunohistochemistry. Two independent experiments; n = 6 mice/group. (E) Osx-mCherry cells and Ocn-Topaz cells were isolated from the OsxCre-mCherry;OcnCre-Topaz double transgenic mice by flow cytometry and expression of the indicated Notch ligands was assessed by qPCR. Experiment performed twice; n = 3/experiment. Data show mean ± SEM. (F) Gene set enrichment analysis (GSEA) comparing Ly6D⁻ CLP versus MPP microarray data. Experiment performed twice; n = 3/experiment. (G) GSEA comparing Ly6D⁻ CLP microarray data obtained from OcnCre;iDTR control versus mutant mice. Experiment was performed twice independently; n = 3–4/experiment.

These data argue against an altered thymic microenvironment (or metabolic milieu) induced by the deletion of Ocn⁺ cells or DT administration as the basis for altered T cell differentiation. They also argue against, but cannot definitively exclude, secondary effects of stress on the lymphopoietic phenotype.

Examining whether the thymocyte production defects were cell autonomous, we adoptively transferred 3 × 10^4 Ly6D⁻-CLPs cells from bone marrow of control or Ocn⁺ cell depleted animals intrathymically into WT mice. After 3 wk, no evidence for a defect in the thymocyte maturation sequence was observed for cells derived from the context of the Ocn⁺ cell–depleted bone marrow (Fig. 9 A). The reversal of abnormalities in all T-intermediate stages in the thymus also led to fully restored mature CD4⁺ and CD8⁺ populations in the bone marrow (Fig. 9 A). Similar results were observed using Lin⁻Sca⁺Kit⁺Flt3⁺ cells. No extrathymic development was observed in organs, including bone marrow, spleen, lymph node, and intestine. Therefore, the perturbation of T cell development induced by Ocn⁺ cell depletion appears to be in enabling bone marrow thymus-seeding cell formation and migration, not in impaired differentiation capacity of cells once they arrive in the thymus.

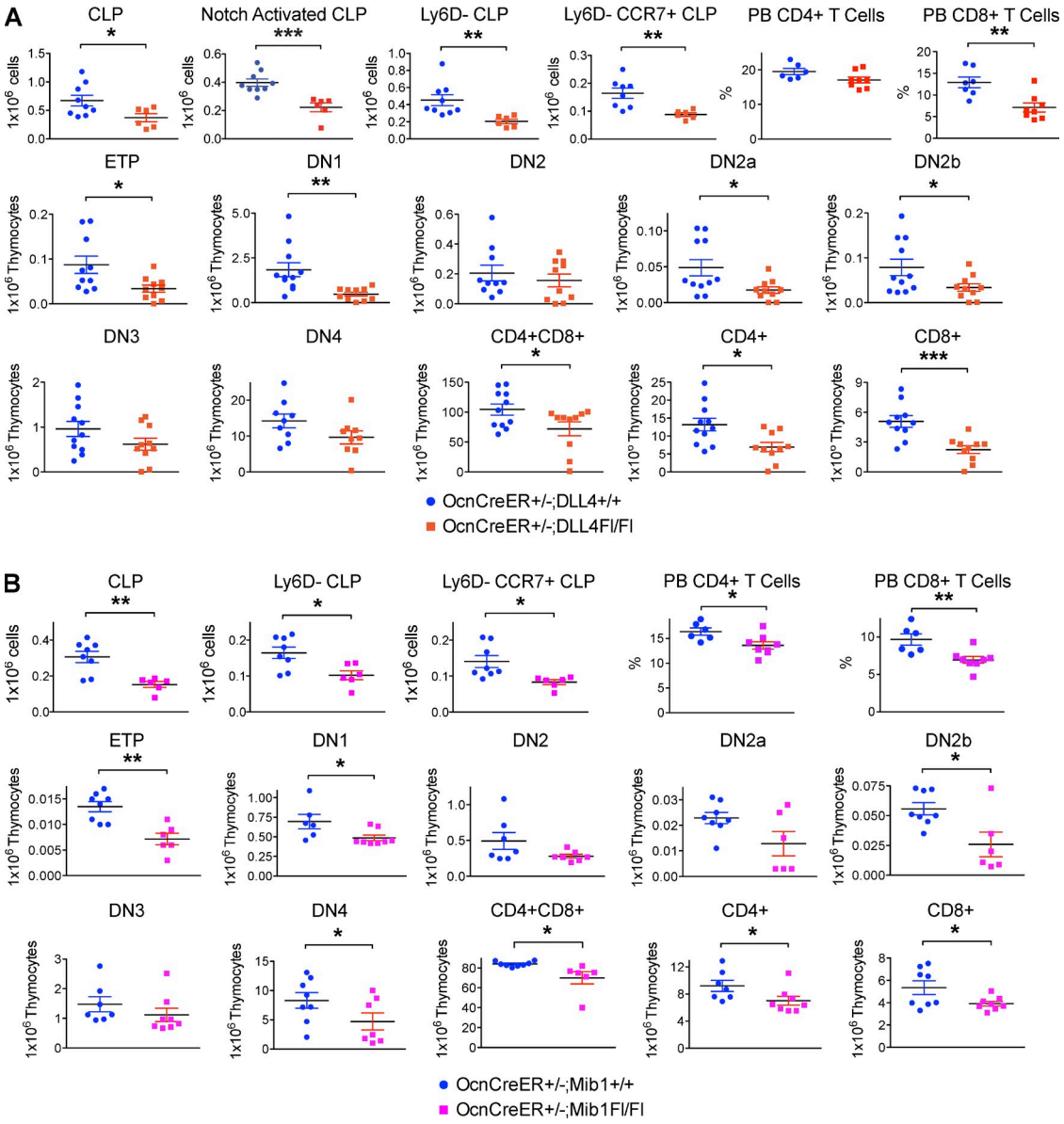

Figure 6. Conditional deletion of DLL4 or Notch ligands in Ocn⁺ cells impaired T lymphopoiesis. (A) OcnCreER$^{+/-}$;Dll4$^{Fl/Fl}$ mutants and OcnCreER$^{+/-}$;Dll4$^{+/+}$ control littermates were injected with 2mg 4-OH-tamoxifen/15 g BW eight times over 4 wk to induce deletion of the DLL4 ligand. Mice were harvested immediately after 4 wk of deletion and bone marrow CLPs, thymic T cell progenitors, and peripheral blood mature T cells were enumerated by flow cytometry. Experiment was performed 3 times independently; *n* = 9–10 mice/group. Data show mean ± SEM. (B) OcnCreER$^{+/-}$;Mib1$^{Fl/Fl}$ mutants and OcnCreER$^{+/-}$;Mib1$^{+/+}$ control littermates were injected with 2 mg 4-OH-tamoxifen/15 g BW 8 times over 4 wk to induce deletion of the *Mib1* gene. Mice were harvested immediately after 4 wk of deletion and bone marrow CLPs, thymic T cell progenitors, and peripheral blood mature T cells were enumerated by flow cytometry. Experiment was performed twice independently; *n* = 6–8 mice/group. Data show mean ± SEM.

Because Notch has been reported to mediate the expression of chemokine receptors in T cell leukemia (Mirandola et al., 2012), we assessed whether OcnCre$^{+/-}$;iDTR bone marrow cells properly express the chemokine receptors (Krueger et al., 2010) or ligands (Sultana et al., 2012) necessary for thymic seeding. We observed modestly decreased CCR7 expression intensity in the CLPs without changes in CCR9 or PSGL1, but with a significant decrease in the number of CCR7^{+}CLP and PSGL1^{+}CLP (Fig. 9 B). CCR7^{+}CLP was also decreased in OcnCreER$^{+/-}$;DLL4$^{-/-}$, OcnCreER$^{+/-}$;Mib1$^{-/-}$, Mx1Cre$^{+/-}$;Pofut1$^{-/-}$, Mx1Cre$^{+/-}$;RBPjk$^{-/-}$ mice, and γ-secretase injected femurs compared with littermate controls (Figs. 6–8). Together, these data indicate that Ocn^{+} cell depletion results in decreased thymic-seeding progenitors and in decreased production of the thymic homing molecule, CCR7, in those progenitors.

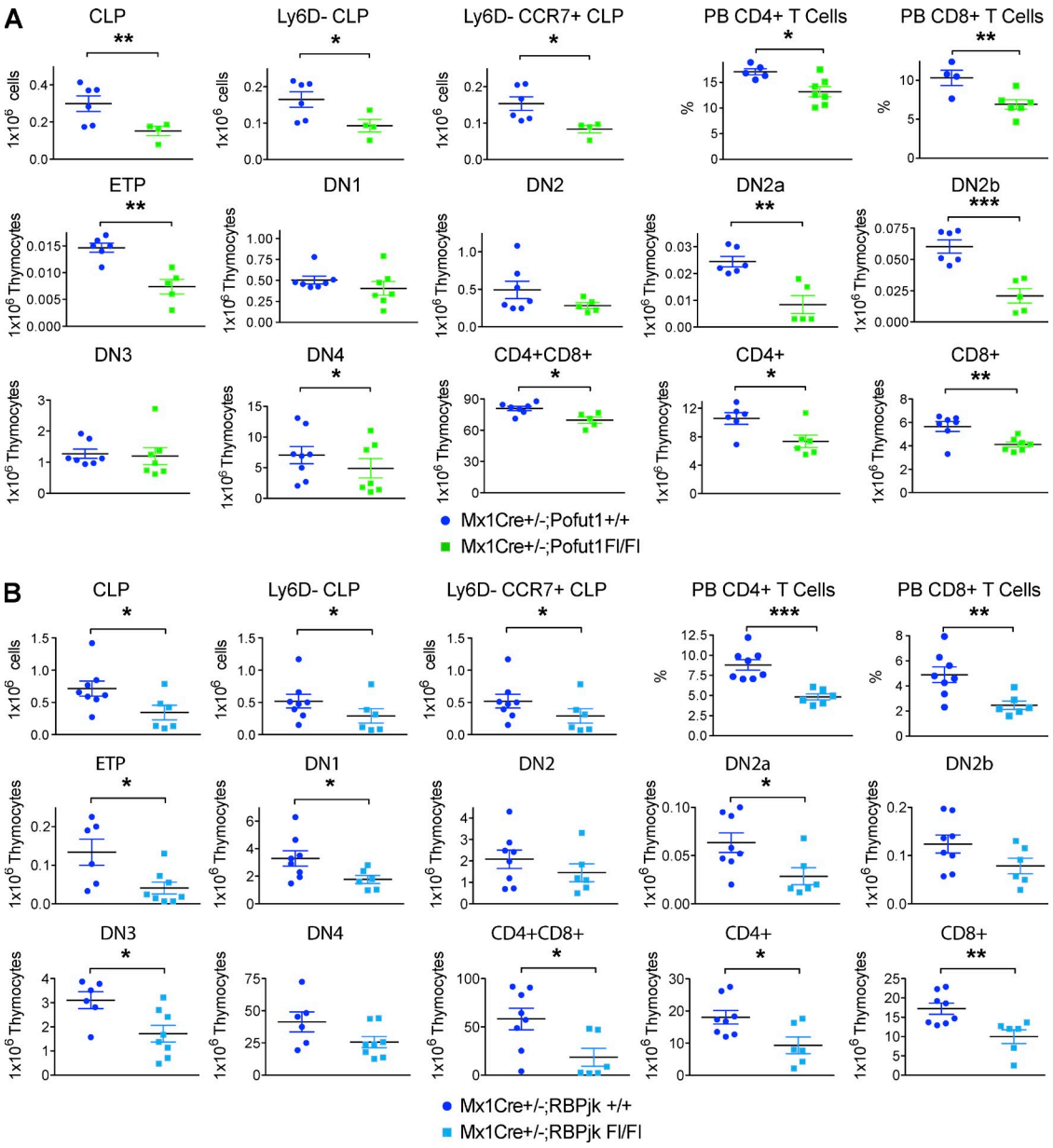

Figure 7. Conditional ablation of Notch signaling in hematopoietic cells impaired T lymphopoiesis. (A) Mx1Cre$^{+/-}$;Pofut1$^{Fl/Fl}$ mutants and Mx1Cre$^{+/-}$;Pofut$^{+/+}$ control littermates were injected with 12.5 µg/g BW polyinosinic:polycytidylic acid (poly(I:C)) every alternate day for 7 d to induce deletion of the *Pofut1* gene. Mice were harvested 4 wk after injection and bone marrow CLPs, thymic T cell progenitors, and peripheral blood mature T cells were enumerated by flow cytometry. Experiment was performed twice independently; n = 4–6 mice/group. Data show mean ± SEM. (B) Mx1Cre$^{+/-}$;RBPjk$^{Fl/Fl}$ mutants and Mx1Cre$^{+/-}$;RBPjk$^{+/+}$ control littermates were injected with 12.5 µg/g BW poly(I:C) every alternate day for 7 d to induce deletion of RBP-Jκ. Mice were harvested 4 wk after injection and bone marrow CLPs, thymic T cell progenitors, and peripheral blood mature T cells were enumerated by flow cytometry. Experiment was performed twice independently; n = 6–8 mice/group. Data show mean ± SEM.

To test whether thymus migratory capacity of bone marrow cells was reduced in vivo, we conducted competitive homing experiments. LKS Flt3$^+$ cells (1.5 × 10^4) or CLPs (two doses: 3.5 × 10^4 or 10^4) from control or Ocn$^+$ cell-depleted mice were isolated, stained with distinctive fluorescent tags, and intravenously injected at a 1:1 ratio into SJL recipients (Fig. 9 C). In parallel, equivalent cells sorted from age matched CCR7$^{-/-}$ mice labeled with a distinctive fluorescent tag were used as positive controls for homing defective cells and similarly competed in a 1:1 ratio into recipients. Recipient thymi were evaluated 24 h after transplant. OcnCre$^{+/-}$;iDTR mutant or CCR7$^{-/-}$ donor cells were similarly compromised in thymic homing ability compared with controls (Fig. 9 C). These data suggest that the reduction in thymocytes may be due to failure to generate thymic-homing competent cells in the bone marrow of Ocn$^+$ cell

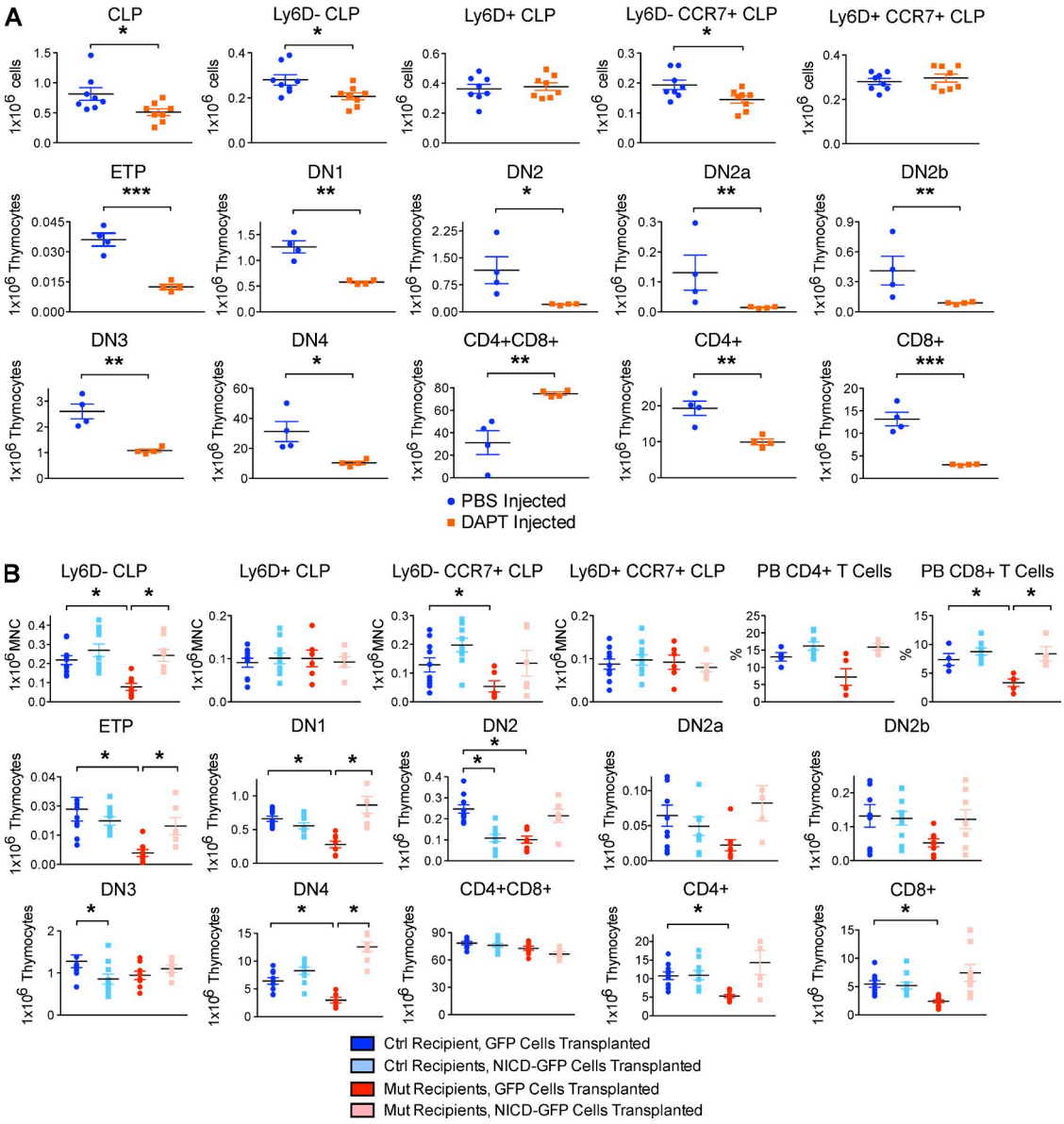

Figure 8. Notch blockade in the bone marrow by γ-secretase inhibitor impaired thymic T cell development, whereas Notch overexpression rescued T lymphoid defect. (A) 2.5 mM DAPT or PBS was injected into the left femur of each of 8 C57BL/6J mice at day −12, −9, −6. At day 0, the left femur, thymus, and peripheral blood were harvested for enumeration of bone marrow CLPs, thymic T cell progenitors, and peripheral blood mature T cells by flow cytometry. Experiment was performed twice independently; n = 4–8 mice/group. Data show mean ± SEM. (B) 10^6 Lineage-depleted hematopoietic progenitors were flow sorted from poly(I:C)-induced Mx1Cre;LSL-NICD-GFP mice or Mx1Cre;LSL-GFP control mice and transplanted into either OcnCre;iDTR mutant or control recipients. Recipients were harvested 1 wk after transplant and bone marrow CLPs, thymic T cell intermediates, and mature peripheral blood T cells were analyzed by flow cytometry. Experiment was performed twice independently; n = 8 mice/group. Data show mean ± SEM.

deleted animals. The defect in homing capacity may be caused by decreased CCR7 or PSGL1 or the combination of the two in the absence of Ocn$^+$ cells in the bone marrow.

To test our hypothesis that Ocn$^+$ cells instruct early T-lineage specification in bone marrow through DLL4, we injected the Ocn$^+$ cell–depleted animals with recombinant mouse DLL4. Although this ligand is generally cell associated, it has been shown by others to induce Notch activation when administered as a recombinant protein (Androutsellis-Theotokis et al., 2006; Benedito et al., 2012; Moya et al., 2012). Control and mutant OcnCre$^{+/-}$;iDTR mice were treated with daily DT injections from day −19. At day −5, mutant OcnCre$^{+/-}$;iDTR mice were co-injected with either 100 ng/g BW or 1 µg/g BW of DLL4 intravenously. All mice were harvested at day 0. Results showed that injection of a high concentration of DLL4 into the bloodstream rescued the OcnCre$^{+/-}$;iDTR bone marrow CLP and increased CCR7 expression on CLPs (Fig. 10 A)

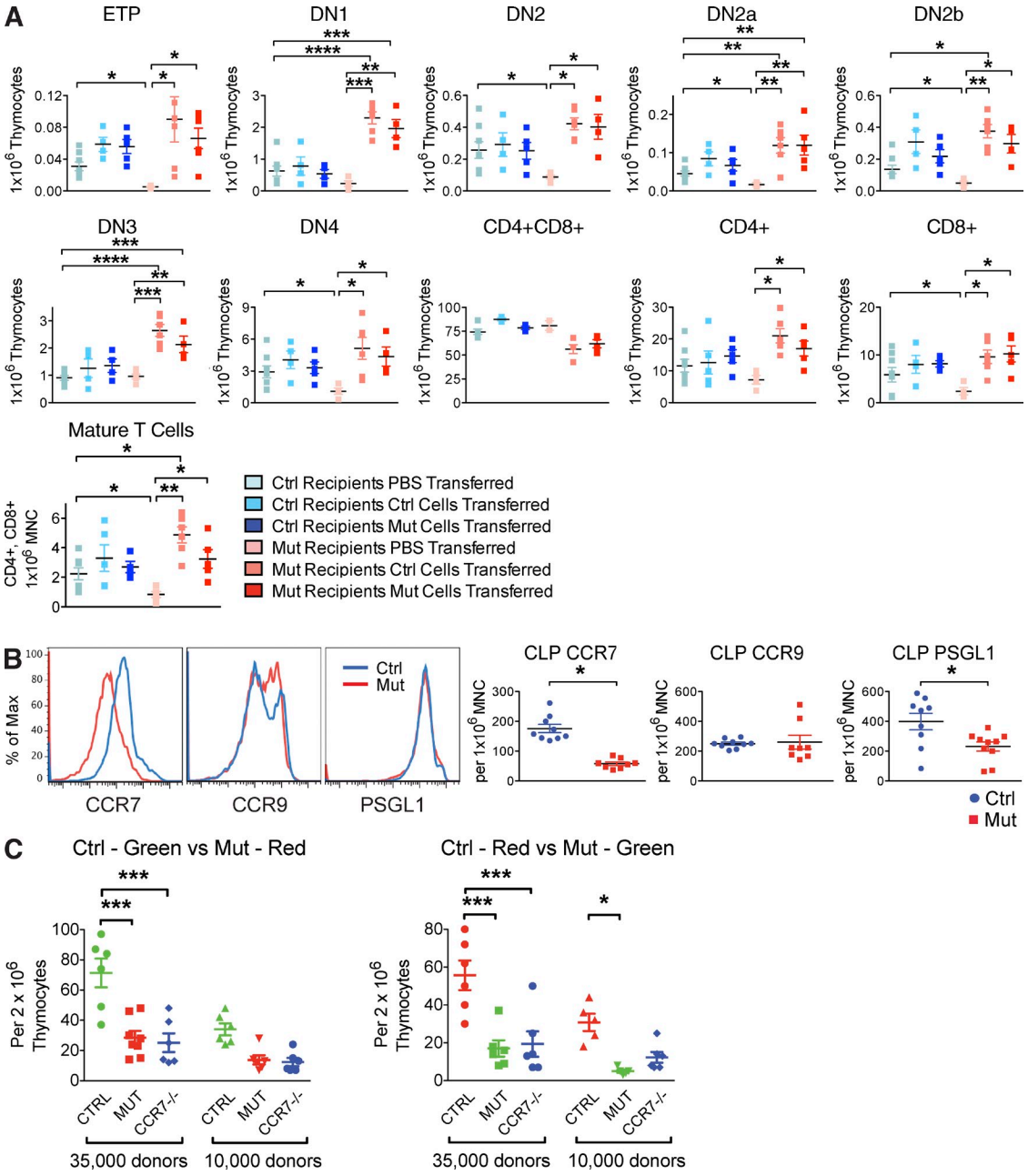

Figure 9. Ocn⁺ cell–depleted animals had intact thymic function but impaired CLP homing ability. (A) 30,000 flow sorted bone marrow CLPs from diphtheria treated OcnCre$^{+/-}$;iDTR animals (Mut) or controls (Ctrl) were injected into the thymus of either OcnCre$^{+/-}$;iDTR DT treated (Mut) or control (Ctrl) animals. Injection of PBS served as mock controls. Thymic T progenitor and mature populations were assessed after 4 wk. Two independent experiments; n = 4–6 mice/group. Data show mean ± SEM. (B) CCR7, CCR9, and PSGL1 cell surface expression on CLP from Ocn⁺ cell–depleted or control mice was assessed by flow cytometry. Panels on the left show expression levels (indicated by fluorescent intensity on the y axis) and dot plots on the right show numbers of cells with positive expression. Minimum two independent experiments; n = 8–10 mice/group. Data show mean ± SEM. (C) CLPs from diphtheria-treated OcnCre;iDTR control and mutant mice were labeled with green and red fluorescent dyes, respectively, mixed in a 1:1 ratio and transplanted intravenously into congenic SJL recipients, and harvested 24 h after transplant. Equal number of CLPs harvested from CCR7$^{-/-}$ mice was used as another control and competed with OcnCre;iDTR mutant CLPs in a similar manner. Donor-derived cells were enumerated from recipient thymi 24 h after transplant. Experiment was repeated with reciprocal dye to control for dye labeling efficiency. 2 independent experiments; n = 10 mice/experiment. Data show mean ± SEM.

and subsequent thymic T cell development (Fig. 10, B–K), resulting in normalized mature T number in the bone marrow (Fig. 10 L). Supplement of a low concentration of DLL4 only partially increased bone marrow CLP (Fig. 10 A), but restored all subsequent stages of T development downstream in the thymus (Fig. 10, B–K). These data are consistent with

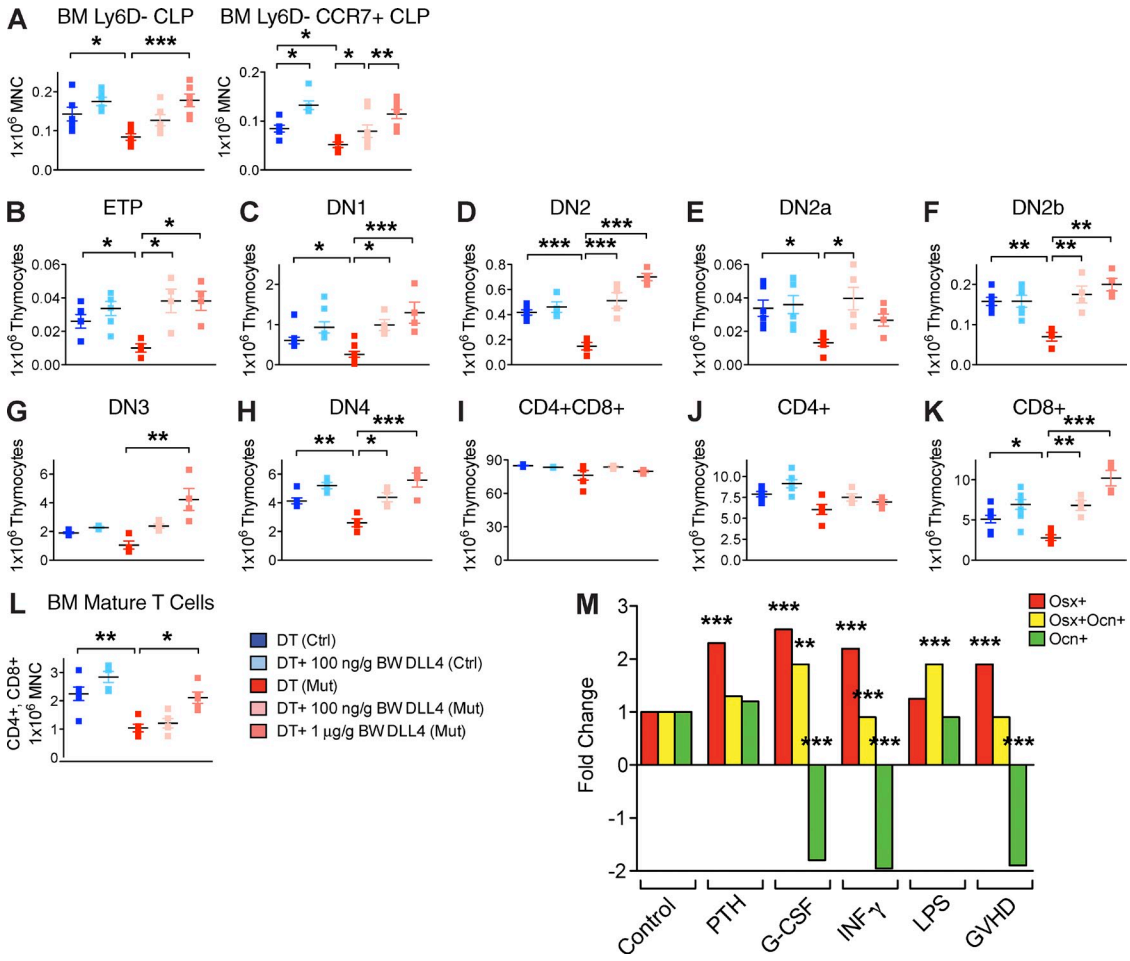

Figure 10. In vivo rescue of T lineage defect by intravenous infusion of DLL4. (A–L) OcnCre;iDTR control and mutant mice were first treated with DT for 21 d to induce Ocn$^+$ cell deletion, then injected with recombinant DLL4 intravenously at two different dosages: 100 ng/g BW or 1 µg/g BW. Flow cytometric evaluation of effects on the number of bone marrow CLPs (A), thymic T cell intermediates (B–K), and mature T cells circulated back to the bone marrow (L). Experiments was performed twice independently; n = 6–12 mice/group. Data show mean ± SEM. (M) Transgenic mice with osteolineage cells at the progenitor stage (Osx$^+$) labeled red, intermediate stage (Osx$^+$Ocn$^+$) labeled yellow, and mature stage (Ocn$^+$) labeled green were treated with either saline control (CNTR), parathyroid hormone (PTH), granulocyte colony-stimulating factor (G-CSF), IFN-γ, LPS, or transplanted in a noncompatible setting to elicit graft-versus-host disease (GvHD). The number of Osx$^+$, Osx$^+$Ocn$^+$, and Ocn$^+$ cells in femurs were enumerated by FACS. Experiment was performed twice; n = 8 mice/experiment. Results are means ± SEM.

DLL4 acting at the level of both the bone marrow and thymus. The impact of DLL4 was both in cell number and CCR7 expression in the bone marrow consistent with a role in both processes.

DISCUSSION

Immune reconstitution after allogeneic hematopoietic stem cell transplantation is a major clinical problem resulting in significant patient morbidity and mortality. We tested whether the number of Ocn$^+$ cells might be compromised in vivo under settings related to hematopoietic stem cell transplantation. We generated mice that simultaneously label Osx-expressing cells and Ocn-expressing cells with distinct fluorescence markers and enumerated the cells by flow cytometry. A specific and marked reduction of Ocn$^+$ cells was observed in a model of allogeneic transplantation and graft-versus-host disease (GvHD), a particularly immunosuppressive clinical scenario and one where T cell reconstitution is markedly delayed. We also noted that granulocyte colony-stimulating factor (G-CSF), commonly used after transplantation, adversely affected Ocn$^+$ cells as did γ-interferon, a cytokine associated with immune activation with infection or GvHD (Fig. 10 M). These data suggest that the context of allogeneic hematopoietic stem cell transplantation may adversely affect critical components of the niche for full immunological reconstitution.

These studies indicate that Ocn$^+$ bone cells may enable T-lineage competent cell production and thymus seeding through expression of DLL4. Although DLL4 is well defined as necessary to enforce T-lineage differentiation in the thymus and cells of multipotency are present in the thymus (Hozumi et al., 2008; Koch et al., 2008; Mohtashami et al., 2010), the data here suggest a contribution of bone cells and bone marrow to

robust T-lymphopoiesis in young adult animals. Other studies of modifying bone cell CCL12 production or deletion of DMP-1$^+$ cells have indicated, respectively defects in CLP (but not mature T cells) or of thymus, T cells, and B cells and metabolism broadly (Ding and Morrison, 2013; Greenbaum et al., 2013; Sato et al., 2013). The lack of T cell phenotype in our OsxCre$^{+/-}$;iDTR model was unexpected and there could be several explanations. Differences in Cre deletion efficiency could be one reason, as we achieved ∼50% cell deletion in the OsxCre$^{+/-}$;iDTR model compared with 70% deletion in the OcnCre$^{+/-}$;iDTR system. Second, the relative balance of Osx$^+$ cells versus Ocn$^+$ cells in the bone marrow may be important for creating a B versus T-progenitor niche. Systemic or indirect effects imposed by Osx$^+$ or Ocn$^+$ cell deletion also remains possible. Based on our current data, we present a model where a specific Notch-ligand, produced by a specific subset of bone cells drive T-lineage competence and enable thymus-seeding cell production. This model may inform strategies to improve T-lineage production and reconstitution in settings of disease, particularly because the bone cells involved appear to be susceptible to loss in contexts like transplantation where T cell generation is of great clinical consequence.

MATERIALS AND METHODS

Mouse models. All single transgenic mouse strains were maintained in a C57BL/6J background by backcrossing to C57BL/6J for at least 10 backcrosses. To specifically delete mature osteolineage cells, the OC-*cre* strain (from T.L. Clemens, Johns Hopkins University, MD; Zhang et al., 2002), which expressed Cre under the *Osteocalcin* promoter was crossed to the iDTR strain (Buch et al., 2005). Temporally controlled cell ablation was achieved upon injection of DT into the OcnCre$^{+/-}$;iDTR strain. Similarly, Osx$^+$ cell deletion was achieved by crossing the Osx1-GFP::Cre mouse (Rodda and McMahon, 2006) to the iDTR strain. To study the effect of Ocn$^+$ cells on hematopoiesis, OcnCre$^{+/-}$ injected with DT or OcnCre$^{+/-}$;iDTR injected with PBS served as controls while OcnCre$^{+/-}$;iDTR injected with DT were used as mutants. For osteoprogenitor deletion, control mice were OsxCre$^{+/-}$ injected with DT or OsxCre$^{+/-}$;iDTR injected with PBS, whereas OsxCre$^{+/-}$;iDTR injected with DT served as mutants. For most experiments, 25 ng DT in PBS/g of body weight was injected daily into both control and mutant animals for 28 d from 4 wk of age to achieve an acute deletion of specific osteolineage populations. Mice were harvested for analysis the next day after the last dose of diphtheria injection. Notch ligand inactivation in Ocn$^+$ cells was achieved by crossing the Ocn-CreER strain (Park et al., 2012) with *Dll4*$^{lox/lox}$ strain (K. Hozumi, Tokai University, Kanagawa, Japan; Hozumi et al., 2008) and with *Mib1*$^{F/F}$ strain (Koo et al., 2005; OcnCreER;DLL4$^{Fl/Fl}$ and OcnCreER;Mib1$^{Fl/Fl}$). Mouse models of Notch inactivation in hematopoietic cells was achieved by crossing the B6.Cg-Tg(Mx1-Cre)1Cgn/J (Mx1-Cre; The Jackson Laboratory) strain with *Pofut1*$^{F/F}$ (Y.-Y. Kong, Seoul National University, Seoul, Republic of Korea; Shi and Stanley, 2003) and RBP-J$^{f/f}$ (T. Honjo, Kyoto University, Kyoto, Japan; Han et al., 2002) strains (Mx1Cre;Pofut1$^{Fl/Fl}$ and Mx1Cre;RBPjk$^{Fl/Fl}$). Mouse strains Gt(ROSA)26Sortm1(Notch1)Dam/J (LSL-NICD-GFP), B6.129X1-Gt(ROSA)26Sortm1(EYFP)Cos/J (LSL-GFP), and C57BL/6-Tg(BGLAP-Topaz)1Rowe/J (OcnCre-Topaz) were obtained from The Jackson Laboratory. OsxCre-mCherry;OcnCre-Topaz was generated by crossing Osx-CreER (Park et al., 2012), Rosa-LSL-mCherry (The Jackson Laboratory), and OcnCre-Topaz strains. For all experiments, littermates were used as controls. C57BL/6J and B6.SJL-*Ptprc*^{a}*Pepc*^{b}/BoyJ (SJL) strains were obtained from The Jackson Laboratory. All animal usage and procedures performed were approved by the Institutional Animal Care and Use Committee of Massachusetts General Hospital.

Bone histology. Tibiae were fixed in 70% ethanol and embedded without demineralization in methyl methacrylate for histomorphometric analysis. 5-µm sections were stained with toluidine blue to quantify static parameters, including bone volume per tissue volume, trabecular number, trabecular separation, osteoblast and osteocyte number per tissue area, and osteoclast number per bone perimeter. Unstained sections were used to measure dynamic parameters, including bone formation rate per tissue volume. A sampling site with an area of ∼1.4 mm^2 was established in the secondary spongiosa of the metaphysis at 450 µm below the growth plate. A standard histomorphometric analysis was performed using the OsteoMeasure system (Osteometrics, Inc.) and the results were expressed according to standardized nomenclature (Parfitt et al., 1987). Statistical analysis was achieved using the nonparametric Mann-Whitney test (n = 7–8). For paraffin sections, femurs and tibiae were collected and fixed in 4% paraformaldehyde overnight, decalcified by 20% EDTA for 1 wk, washed in PBS, dehydrated through a series of alcohol changes up to 70% EtOH, and embedded in paraffin. Paraffin sections were stained with hematoxylin and eosin for general morphology, as well as von Kossa and Goldner trichrome. Tartrate-resistant acid phosphatase (TRAP) staining was used to reveal osteoclasts. Alteration of osteoblastic activity was assessed by measuring serum levels of osteocalcin and N-terminal propeptide of type I procollagen (P1NP) using RatLaps ELISA kits (n = 22–24). Changes in osteoclastic bone resorption was assessed by measuring the C-terminal telopeptides of collagen type I fragments in mouse serum using RatLaps EIA kit (n = 22–24).

Immunohistochemistry. Expression of the DT receptor on cell surface was detected by immunohistochemical staining of paraffin sections with anti–human heparin-binding EGF-like growth factor (anti–hHB-EGF) antibody (R&D Systems; AF-259-NA). In brief, deparaffinized and rehydrated sections were treated with 0.1% trypsin for antigen unmasking and 3% H_2O_2 to block endogenous peroxidase activity. Sections were then blocked with reagent containing 5% animal serum in PBS-T for 1 h. Goat polyclonal anti–hHB-EGF antibody was used at 1:25 dilution, coupled with horse biotinylated anti–goat IgG secondary antibody (Vector Lab) at 1:400 dilution. Rabbit polyclonal anti-DLL4 antibody (Abcam; ab84081) was used at a 1:50 dilution, coupled with biotinylated anti–rabbit antibody at 1:250 dilution (Vector Lab). After antibody staining, sections were washed in PBS-T, treated with VECTASTAIN ABC kit for biotin-streptavidin signal amplification, and subsequently visualized by DAB Peroxidase Substrate kit. Phycoerythrin-conjugated anti-PECAM1 antibody (BD) was applied at 1:100 dilution and mounted with DAPI containing mounting medium. Ocn expressing mature osteoblasts and osteocytes were recognized by goat polyclonal anti-osteocalcin antibody (Santa Cruz Biotechnology, Inc.; sc-18322) at 1:50 dilution followed by donkey anti–goat IgG secondary antibody conjugated to Alexa Fluor 488 at 1:1,000 dilution. Green fluorescent osteocalcin-antibody stainings were individually superimposed with red fluorescent TUNEL (In situ Cell Death Detection kit TMR Red; Roche) staining.

Colony forming unit–osteoblast (CFU-Ob) assay. Bone marrow cells were collected from each mouse by flushing end-excised femurs and tibiae with PBS containing penicillin and streptomycin. Collected bone marrow cells were incubated with ACK lysis buffer to remove red blood cells, washed with PBS, and plated at 10^7 cells per well in a 6-well plate supplemented with DMEM and 10% FBS. Nonadherent cells were removed on the fifth day and adherent cells were replated at 5×10^6 cells per well and cultured in the same media until confluent. Once cultures reached confluency, medium was changed into DMEM containing 50 µg/ml ascorbic acid, 10^{-8} M dexamethasone, and 8 mM β-glycerophosphate and changed every 2–3 d to induce osteogenic differentiation. 14 d later, cultures were fixed in 4% PFA, and stained with 0.5% Alizarin Red for visualization of mineralized nodules with brightfield microscopy. Cells were plated in triplicates and assay was repeated three times.

Flow cytometry. Before sacrifice, peripheral blood was collected from each mouse and subjected to complete blood cell count. For each mouse, tibiae, femurs, iliac crests, spines, ulnae, radii, and humeri were collected for bone marrow cells. In addition, spleen and thymus were also collected for lymphocyte staining. Changes in hematopoietic populations were quantified by flow cytometry. Bone marrow cells harvested from each animal were counted. We routinely stained 5×10^7 cells per sample for the hematopoietic stem population, and 10^7 cells per sample for each progenitor and mature population. Lineage cocktail consists of biotinylated B220, CD3e, CD4, CD8a, CD19, CD11b, Gr1, Ter119, CD11c, and NK1.1 antibodies. Fluorescence conjugated to streptavidin was used to recognize lineage cocktail. The following antibody combinations were used to recognize different hematopoietic populations: hematopoietic stem and progenitor cells (Lineage-Pacific Orange, Sca-Pacific Blue, cKit-APC-Cy7, CD48-APC, CD150-PE-Cy7), CLP (Lineage-Pacific Orange, Sca-Pacific Blue, cKit-APC-Cy7, CD127-PE-Cy7, Thy1.2-FITC, Ly6D-APC), GMP, CMP and MEP (Lineage-Pacific Orange, Sca-Pacific Blue, cKit-APC-Cy7, CD34-FITC, CD16/32-PE-Cy7), B cells (B220-APC), mature T cells (CD4-Pacific Blue, CD8-APC), monocytes (CD11b-APC), granulocytes (Gr1-FITC), erythroid cells (CD45-APC, Ter119-PE), megakaryocytes (CD41-APC). For thymic T cell development, we used: CD25-FITC, CD44-PE, cKit-APC-Cy7, CD4-Pacific Blue, CD8-APC. Ki67-FITC and DAPI staining were coupled with staining of any specific populations to reveal cell cycle status, while Annexin V and 7-AAD staining were used for apoptotic analysis.

Transplantation. For transplantation of WT hematopoietic cells into Ocn+ cell depleted mutant environment, 1×10^6 bone marrow mononuclear cells from 6-wk-old SJL donors were transplanted into each of 10 age-matched 9.5 Gy lethally irradiated $OcnCre^{+/-}$ control or $OcnCre^{+/-}$;iDTR mutant recipients. DT administration into both control and mutant recipients began at 4 wk before transplantation and were maintained every alternate day until 16 wk after transplantation. Recipients were bled at 8, 12, 16 wk after transplantation. Peripheral blood was subjected to complete blood cell count and stained for CD45.1-PE, CD45.2-APC to measure donor reconstitution by flow cytometry. At 16 wk after transplantation, all recipients were sacrificed. Bone marrow cells were harvested from femurs, tibiae, iliac crests, and red blood cell, and then lysed and stained with CD45.1-PE, CD45.2-APC, Mac1-APC, Gr1-FITC, B220-APC, CD4-APC, and CD8-FITC antibodies to measure reconstitution by individual lineages using flow cytometry.

To competitively transplant bone marrow hematopoietic cells from $OcnCre^{+/-}$;iDTR animals into WT recipients, 5×10^5 bone marrow mononuclear cells from 6-wk-old mutant $OcnCre^{+/-}$;iDTR or control $OcnCre^{+/-}$ donors were competed with 5×10^5 bone marrow mononuclear cells from age-matched congenic SJL donors. For both control and donor group, a total of 10^6 mixed donor cells were transplanted into each of 10 age-matched 9.5 Gy irradiated SJL recipients. Recipients were bled at 8, 12, and 16 wk after transplantation. Peripheral blood was subjected to complete blood cell count and stained with CD45.1-PE, CD45.2-APC antibodies for donor reconstitution readout by flow cytometry. At 16 wk after transplantation, all recipients were sacrificed. Red blood cells were lysed and total bone marrow cells were stained with CD45.1-PE, CD45.2-APC, Mac1-APC, Gr1-FITC, B220-APC, CD4-APC, and CD8-FITC antibodies to measure lineage reconstitution by flow cytometry.

Microarrays. Osx^+, Osx^+Ocn^+, and Ocn^+ cells were sorted at 6 d after tamoxifen injection from 4–6-wk-old OsxCre-mCherry;OcnCre-Topaz mice using FACSAria (BD). $Ly6D^-$ CLPs were sorted from 6–8 wk old OcnCre;iDTR mutants and controls using the FACSAria after daily DT treatment for 4 wk. RNA was extracted using TRIzol (Invitrogen) according to the manufacturer's instructions. Samples were processed by the NuGen Ovation V2 laboratory process in the microarray core facility of the Dana Farber Cancer Institute. In brief, first stand cDNA was prepared from total RNA using a DNA/RNA chimeric primer and a reverse transcription. The resulting double stranded cDNA with a unique heteroduplex at the 5′ end of the antisense strand were amplified using SPIATM amplification, a repeated process of SPIATM DNA/RNA primer hybridization, DNA replication, strand displacement and RNA cleavage which resulted in a rapid accumulation of cDNA with sequence complementary to the original RNA. The SPIATM amplified cDNA was purified using the Zymo Research DNA Clean & Concentrator system. The purified cDNA was fragmented through a chemical and enzymatic process and labeled via enzymatic attachment of a biotin-labeled nucleotide to the 3′-hydroxyl end of the fragmented cDNA. The biotinylated cDNA was added to a hybridization solution containing several biotinylated control oligonucleotides (for quality control), and hybridized to the Mouse430A microarray chip overnight at 45°C. The chips were then transferred to a fluidics instrument that performs washes to remove cDNA that has not hybridized to its complementary oligonucleotide probe. The bound cDNA was then fluorescently labeled using phycoerythrin-conjugated streptavidin (SAPE); additional fluors were then added using biotinylated anti-streptavidin antibody and additional SAPE. Each cDNA bound at its complementary oligonucleotide was excited using a confocal laser scanner, and the positions and intensities of the fluorescent emissions were captured. These measures provide the basis of subsequent biostatistical analysis. Standard QA/QC analyses involved chip analysis with the assay QualityMetrics BioConductor package and found no significant quality issues with any of the chips, as determined by (among other methods) visual inspection, intensity distributions, or RNA degradation plots. The data were background corrected and normalized with RMA (Robust Multichip Average) using the "affy" BioConductor package. Values in the data matrix represent log2 normalized intensity values.

All microarray datasets have been deposited in NCBI's Gene Expression Omnibus (GEO) and are accessible through GEO Series accession nos. GSE66042 and GSE66102.

Quantitative PCR. Flow sorted cells were extracted for RNA using the RNAqueous-4PCR kit (Ambion). Flushed and crushed femoral bones of mutant or control animals were used for RNA extraction by TRIzol. Quantitative PCR were performed with TaqMan probes using the expression of the housekeeping GAPDH gene for normalization.

Competitive thymic homing experiment. 35,000 or 10,000 Ly6D- CLPs ($Lin^-Sca^+cKit^+IL7R^+Thy1.2^-Ly6D^-$) were sorted from OcnCre;iDTR control and mutant donors (CD45.2-Pacific Blue), labeled with 10 µM CFDA-SE (Invitrogen) and 1 µg/ml VivoTag680 (VT680, VisEn Medical), respectively, mixed in a 1:1 ratio, and transplanted into each congenic SJL recipient (CD45.1-PE) by retro-orbital injection. The same number of progenitor cells sorted from $CCR7^{-/-}$ mice served as another control to compete with OcnCre;iDTR mutant donors. Recipient thymi were harvested 24 h after transplant and donor-derived cells (CD45.2-Pacific Blue) from OcnCre;DTR control (CFDA-SE) and mutant (VT680) were enumerated by flow cytometry. To account for differential dye-labeling efficiency, the experiment was repeated with the competing cells stained with reciprocal dyes, mixed in equal ratio, and transplanted into SJL mice in the same manner. Experiment was also performed using 15,000 sorted $Lin^-Sca^+cKit^+Flt3^+$ hematopoietic progenitors as donor cells.

Intrathymic adoptive transfer assay. We follow the procedure described previously (Goldschneider et al., 1986) with the following modifications: Mice were anesthetized with intraperitoneal injection of a mixture of ketamine (100 mg/kg) and xylazine (10 mg/kg). Sorted Ly6D-CLP ($Lin^-Sca^+cKit^+IL7R^+Thy1.2^-Ly6D^-$) or $Flt3^+$ LKS ($Lin^-Sca^+cKit^+Flt3^+$) cells (30,000 cells in 20 µl PBS) were injected at two sites in the anterior superior portion of each thymus lobe (10 µl/site) using a Hamilton syringe mounted with a 30-gauge needle. After surgical procedure, mice were placed under the heat lamp for 30 min to aid recovery from anesthesia and were monitored daily for any signs of discomfort after the Pain Assessment Protocol published by the National Research Council (US) Committee. Mice that demonstrated signs of persistent pain were euthanized. Mice were sacrificed on the 14th day after surgery by CO_2 asphyxiation and cervical dislocation, and thymi were harvested for cell analysis by flow cytometry.

DLL4 rescue experiment. Control OcnCre$^{+/-}$ and mutant OcnCre$^{+/-}$;iDTR mice were intraperitoneally injected with 100 ng/g BW DT daily since day −19. Starting from day −5, OcnCre;DTR mutants were co-injected daily with either 100 ng/g BW or 1 µg/g BW of recombinant mouse DLL4 (R&D Systems) intravenously. All mice were harvested at day 0 for bone marrow cells and thymi collection. Bone marrow cells were red blood cell lysed and stained for CLP, CD4, and CD8-specific antibodies, whereas thymocytes were stained for T developmental specific antibodies for flow cytometric analysis. The experiment was repeated twice.

Intratibial injection of DAPT. We injected 10 µl of either 2.5 mM DAPT (EMD Millipore) or PBS as control into the left tibia of each of eight C57BL/6 mice at day −12, −9, and −6, and harvested the left femur, thymus, and peripheral blood at day 0 for flow cytometric analysis.

GvHD model. For the induction of GvHD, 5×10^6 bone marrow cells were mixed with 2×10^6 CD4/CD8$^+$ purified splenic T cells from BALB/c donor mice and injected in Osx-Cre;Rosa-fl-STOP-fl-mCherry;Ocn-GFP triple transgenic recipient mice that had been previously irradiated with 9.5 Gy. Control recipient mice received 5×10^6 bone marrow cells mixed with 2×10^6 CD4/CD8$^+$ splenic T cells from C57BL/6 donor mice. The purification of the CD4/8$^+$ T cells was achieved using the MACS LD cell separation columns and the MACS Streptavidin MicroBeads (Miltenyi Biotec). Mice were monitored for signs of GvHD daily and the degree of clinical GvHD was assessed weekly by a scoring system that sums changes in five clinical parameters: weight loss, posture (hunching), activity, fur texture and skin integrity. 2 wk after the transplantation, mice were sacrificed.

Statistical analysis. Statistical analysis of all paired experiments was analyzed by two-tailed Student's *t* test. All graphs were represented with mean and standard error of the mean, where *, $P < 0.05$; **, $P < 0.01$; ***, $P < 0.001$; and ****, $P < 0.0001$, unless otherwise stated. Statistical comparison of multiple parameters were analyzed by One-way ANOVA, followed by Bonferroni post-test, where *, $P < 0.05$; **, $P < 0.01$; ***, $P < 0.001$; and ****, $P < 0.0001$.

Online supplemental material. Fig. S1 shows flow gating strategies for bone marrow singlets and B cells. Fig. S2 depicts flow gating strategies for bone marrow T cells, monocytes, granulocytes, erythroid cells, and megakaryocytes. Fig. S3 illustrates flow gating strategies for bone marrow hematopoietic progenitor cells. Fig. S4 diagrams flow gating strategies for intrathymic T cells. Fig. S5 describes flow gating strategies for LepR$^+$ cells in the bone marrow stroma. Online supplemental material is available at http://www.jem.org/cgi/content/full/jem.20141843/DC1.

We are grateful to the following investigators for the original generation and sharing of strains: Dr. Thomas L. Clemens (OC-*cre*), Dr. Katsuto Hozumi (*Dll4*$^{lox/lox}$), Dr. Young-Yun Kong (*Mib1*$^{F/F}$), Dr. Pamela Stanley (*Pofut1*$^{F/F}$), and Dr. Tasuko Honjo (RBP-J$^{f/f}$). The authors would like to thank Oliver Hofmann and John Hutchinson of the HSPH Bioinformatics Core, Harvard School of Public Health, Boston, MA for assistance with microarray analysis.

This work was supported by MGH Federal Share of the Program Income under C06 CA059267, Proton Therapy Research and Treatment Center (V.W.C. Yu), BD Biosciences Stem Cell Grant (V.W.C. Yu), Bullock-Wellman Fellowship Award (V.W.C. Yu), Tosteson & Fund for Medical Discovery Fellowship (V.W.C. Yu), NHLBI grants HL097794 (D.T. Scadden), HL044851 (D.T. Scadden), and HL100402 (D.T. Scadden).

The authors declare no competing financial interests.

Submitted: 23 September 2014
Accepted: 26 March 2015

REFERENCES

Androutsellis-Theotokis, A., R.R. Leker, F. Soldner, D.J. Hoeppner, R. Ravin, S.W. Poser, M.A. Rueger, S.K. Bae, R. Kittappa, and R.D. McKay. 2006. Notch signalling regulates stem cell numbers in vitro and in vivo. *Nature*. 442:823–826. http://dx.doi.org/10.1038/nature04940

Awong, G., J. Singh, M. Mohtashami, M. Malm, R.N. La Motte-Mohs, P.M. Benveniste, P. Serra, E. Herer, M.R. van den Brink, and J.C. Zúñiga-Pflücker. 2013. Human proT-cells generated in vitro facilitate hematopoietic stem cell-derived T-lymphopoiesis in vivo and restore thymic architecture. *Blood*. 122:4210–4219. http://dx.doi.org/10.1182/blood-2012-12-472803

Benedito, R., S.F. Rocha, M. Woeste, M. Zamykal, F. Radtke, O. Casanovas, A. Duarte, B. Pytowski, and R.H. Adams. 2012. Notch-dependent VEGFR3 upregulation allows angiogenesis without VEGF-VEGFR2 signalling. *Nature*. 484:110–114. http://dx.doi.org/10.1038/nature10908

Buch, T., F.L. Heppner, C. Tertilt, T.J. Heinen, M. Kremer, F.T. Wunderlich, S. Jung, and A. Waisman. 2005. A Cre-inducible diphtheria toxin receptor mediates cell lineage ablation after toxin administration. *Nat. Methods*. 2:419–426. http://dx.doi.org/10.1038/nmeth762

Ding, L., and S.J. Morrison. 2013. Haematopoietic stem cells and early lymphoid progenitors occupy distinct bone marrow niches. *Nature*. 495:231–235. http://dx.doi.org/10.1038/nature11885

Greenbaum, A., Y.M. Hsu, R.B. Day, L.G. Schuettpelz, M.J. Christopher, J.N. Borgerding, T. Nagasawa, and D.C. Link. 2013. CXCL12 in early mesenchymal progenitors is required for haematopoietic stem-cell maintenance. *Nature*. 495:227–230.

Goldschneider, I., K.L. Komschlies, and D.L. Greiner. 1986. Studies of thymocytopoiesis in rats and mice. I. Kinetics of appearance of thymocytes using a direct intrathymic adoptive transfer assay for thymocyte precursors. *J. Exp. Med*. 163:1–17. http://dx.doi.org/10.1084/jem.163.1.1

Han, H., K. Tanigaki, N. Yamamoto, K. Kuroda, M. Yoshimoto, T. Nakahata, K. Ikuta, and T. Honjo. 2002. Inducible gene knockout of transcription factor recombination signal binding protein-J reveals its essential role in T versus B lineage decision. *Int. Immunol*. 14:637–645. http://dx.doi.org/10.1093/intimm/dxf030

Harman, B.C., W.E. Jenkinson, S.M. Parnell, S.W. Rossi, E.J. Jenkinson, and G. Anderson. 2005. T/B lineage choice occurs prior to intrathymic Notch signaling. *Blood*. 106:886–892. http://dx.doi.org/10.1182/blood-2004-12-4881

Holmes, R., and J.C. Zúñiga-Pflücker. 2009. The OP9-DL1 system: generation of T-lymphocytes from embryonic or hematopoietic stem cells in vitro. *Cold Spring Harb. Protoc*. 2009:pdb.prot5156. http://dx.doi.org/10.1101/pdb.prot5156

Hozumi, K., C. Mailhos, N. Negishi, K. Hirano, T. Yahata, K. Ando, S. Zuklys, G.A. Holländer, D.T. Shima, and S. Habu. 2008. Delta-like 4 is indispensable in thymic environment specific for T cell development. *J. Exp. Med*. 205:2507–2513. http://dx.doi.org/10.1084/jem.20080134

Inlay, M.A., D. Bhattacharya, D. Sahoo, T. Serwold, J. Seita, H. Karsunky, S.K. Plevritis, D.L. Dill, and I.L. Weissman. 2009. Ly6d marks the earliest stage of B-cell specification and identifies the branchpoint between B-cell and T-cell development. *Genes Dev.* 23:2376–2381. http://dx.doi.org/10.1101/gad.1836009

Karsunky, H., M.A. Inlay, T. Serwold, D. Bhattacharya, and I.L. Weissman. 2008. Flk2+ common lymphoid progenitors possess equivalent differentiation potential for the B and T lineages. *Blood*. 111:5562–5570. http://dx.doi.org/10.1182/blood-2007-11-126219

Koch, U., E. Fiorini, R. Benedito, V. Besseyrias, K. Schuster-Gossler, M. Pierres, N.R. Manley, A. Duarte, H.R. Macdonald, and F. Radtke. 2008. Delta-like 4 is the essential, nonredundant ligand for Notch1 during thymic T cell lineage commitment. *J. Exp. Med*. 205:2515–2523. http://dx.doi.org/10.1084/jem.20080829

Koo, B.K., H.S. Lim, R. Song, M.J. Yoon, K.J. Yoon, J.S. Moon, Y.W. Kim, M.C. Kwon, K.W. Yoo, M.P. Kong, et al. 2005. Mind bomb 1 is essential for generating functional Notch ligands to activate Notch. *Development*. 132:3459–3470. http://dx.doi.org/10.1242/dev.01922

Krueger, A., and H. von Boehmer. 2007. Identification of a T lineage-committed progenitor in adult blood. *Immunity*. 26:105–116. http://dx.doi.org/10.1016/j.immuni.2006.12.004

Krueger, A., S. Willenzon, M. Lyszkiewicz, E. Kremmer, and R. Förster. 2010. CC chemokine receptor 7 and 9 double-deficient hematopoietic progenitors are severely impaired in seeding the adult thymus. *Blood*. 115:1906–1912. http://dx.doi.org/10.1182/blood-2009-07-235721

Love, P.E., and A. Bhandoola. 2011. Signal integration and crosstalk during thymocyte migration and emigration. *Nat. Rev. Immunol.* 11:469–477. http://dx.doi.org/10.1038/nri2989

Luche, H., T. Nageswara Rao, S. Kumar, A. Tasdogan, F. Beckel, C. Blum, V.C. Martins, H.R. Rodewald, and H.J. Fehling. 2013. In vivo fate mapping identifies pre-TCRα expression as an intra- and extrathymic, but not prethymic, marker of T lymphopoiesis. *J. Exp. Med.* 210:699–714. http://dx.doi.org/10.1084/jem.20122609

Maeda, T., T. Merghoub, R.M. Hobbs, L. Dong, M. Maeda, J. Zakrzewski, M.R. van den Brink, A. Zelent, H. Shigematsu, K. Akashi, et al. 2007. Regulation of B versus T lymphoid lineage fate decision by the proto-oncogene LRF. *Science.* 316:860–866. http://dx.doi.org/10.1126/science.1140881

Mansson, R., S. Zandi, E. Welinder, P. Tsapogas, N. Sakaguchi, D. Bryder, and M. Sigvardsson. 2010. Single-cell analysis of the common lymphoid progenitor compartment reveals functional and molecular heterogeneity. *Blood.* 115:2601–2609. http://dx.doi.org/10.1182/blood-2009-08-236398

Mirandola, L., M. Chiriva-Internati, D. Montagna, F. Locatelli, M. Zecca, M. Ranzani, A. Basile, M. Locati, E. Cobos, W.M. Kast, et al. 2012. Notch1 regulates chemotaxis and proliferation by controlling the CC-chemokine receptors 5 and 9 in T cell acute lymphoblastic leukaemia. *J. Pathol.* 226:713–722. http://dx.doi.org/10.1002/path.3015

Mohtashami, M., D.K. Shah, H. Nakase, K. Kianizad, H.T. Petrie, and J.C. Zúñiga-Pflücker. 2010. Direct comparison of Dll1- and Dll4-mediated Notch activation levels shows differential lymphomyeloid lineage commitment outcomes. *J. Immunol.* 185:867–876. http://dx.doi.org/10.4049/jimmunol.1000782

Moya, I.M., L. Umans, E. Maas, P.N. Pereira, K. Beets, A. Francis, W. Sents, E.J. Robertson, C.L. Mummery, D. Huylebroeck, and A. Zwijsen. 2012. Stalk cell phenotype depends on integration of Notch and Smad1/5 signaling cascades. *Dev. Cell.* 22:501–514. http://dx.doi.org/10.1016/j.devcel.2012.01.007

Parfitt, A.M., M.K. Drezner, F.H. Glorieux, J.A. Kanis, H. Malluche, P.J. Meunier, S.M. Ott, and R.R. Recker. Report of the ASBMR Histomorphometry Nomenclature Committee. 1987. Bone histomorphometry: standardization of nomenclature, symbols, and units. *J. Bone Miner. Res.* 2:595–610. http://dx.doi.org/10.1002/jbmr.5650020617

Park, D., J.A. Spencer, B.I. Koh, T. Kobayashi, J. Fujisaki, T.L. Clemens, C.P. Lin, H.M. Kronenberg, and D.T. Scadden. 2012. Endogenous bone marrow MSCs are dynamic, fate-restricted participants in bone maintenance and regeneration. *Cell Stem Cell.* 10:259–272. http://dx.doi.org/10.1016/j.stem.2012.02.003

Rodda, S.J., and A.P. McMahon. 2006. Distinct roles for Hedgehog and canonical Wnt signaling in specification, differentiation and maintenance of osteoblast progenitors. *Development.* 133:3231–3244. http://dx.doi.org/10.1242/dev.02480

Rothenberg, E.V., J. Zhang, and L. Li. 2010. Multilayered specification of the T-cell lineage fate. *Immunol. Rev.* 238:150–168. http://dx.doi.org/10.1111/j.1600-065X.2010.00964.x

Sambandam, A., I. Maillard, V.P. Zediak, L. Xu, R.M. Gerstein, J.C. Aster, W.S. Pear, and A. Bhandoola. 2005. Notch signaling controls the generation and differentiation of early T lineage progenitors. *Nat. Immunol.* 6:663–670. http://dx.doi.org/10.1038/ni1216

Sato, M., N. Asada, Y. Kawano, K. Wakahashi, K. Minagawa, H. Kawano, A. Sada, K. Ikeda, T. Matsui, and Y. Katayama. 2013. Osteocytes regulate primary lymphoid organs and fat metabolism. *Cell Metab.* 18:749–758. http://dx.doi.org/10.1016/j.cmet.2013.09.014

Scimone, M.L., I. Aifantis, I. Apostolou, H. von Boehmer, and U.H. von Andrian. 2006. A multistep adhesion cascade for lymphoid progenitor cell homing to the thymus. *Proc. Natl. Acad. Sci. USA.* 103:7006–7011. http://dx.doi.org/10.1073/pnas.0602024103

Shi, S., and P. Stanley. 2003. Protein O-fucosyltransferase 1 is an essential component of Notch signaling pathways. *Proc. Natl. Acad. Sci. USA.* 100:5234–5239. http://dx.doi.org/10.1073/pnas.0831126100

Sultana, D.A., S.L. Zhang, S.P. Todd, and A. Bhandoola. 2012. Expression of functional P-selectin glycoprotein ligand 1 on hematopoietic progenitors is developmentally regulated. *J. Immunol.* 188:4385–4393. http://dx.doi.org/10.4049/jimmunol.1101116

Tan, J.B., I. Visan, J.S. Yuan, and C.J. Guidos. 2005. Requirement for Notch1 signals at sequential early stages of intrathymic T cell development. *Nat. Immunol.* 6:671–679. http://dx.doi.org/10.1038/ni1217

Tsapogas, P., S. Zandi, J. Åhsberg, J. Zetterblad, E. Welinder, J.I. Jönsson, R. Månsson, H. Qian, and M. Sigvardsson. 2011. IL-7 mediates Ebf-1-dependent lineage restriction in early lymphoid progenitors. *Blood.* 118:1283–1290. http://dx.doi.org/10.1182/blood-2011-01-332189

Uhmann, A., J. van den Brandt, K. Dittmann, I. Hess, R. Dressel, C. Binder, F. Lühder, H. Christiansen, M. Fassnacht, A. Bhandoola, et al. 2011. T cell development critically depends on prethymic stromal patched expression. *J. Immunol.* 186:3383–3391. http://dx.doi.org/10.4049/jimmunol.1001939

Visan, I., J.S. Yuan, J.B. Tan, K. Cretegny, and C.J. Guidos. 2006. Regulation of intrathymic T-cell development by Lunatic Fringe- Notch1 interactions. *Immunol. Rev.* 209:76–94. http://dx.doi.org/10.1111/j.0105-2896.2006.00360.x

Visnjic, D., Z. Kalajzic, D.W. Rowe, V. Katavic, J. Lorenzo, and H.L. Aguila. 2004. Hematopoiesis is severely altered in mice with an induced osteoblast deficiency. *Blood.* 103:3258–3264. http://dx.doi.org/10.1182/blood-2003-11-4011

Welinder, E., R. Mansson, E.M. Mercer, D. Bryder, M. Sigvardsson, and C. Murre. 2011. The transcription factors E2A and HEB act in concert to induce the expression of FOXO1 in the common lymphoid progenitor. *Proc. Natl. Acad. Sci. USA.* 108:17402–17407. http://dx.doi.org/10.1073/pnas.1111766108

Wu, J.Y., L.E. Purton, S.J. Rodda, M. Chen, L.S. Weinstein, A.P. McMahon, D.T. Scadden, and H.M. Kronenberg. 2008. Osteoblastic regulation of B lymphopoiesis is mediated by Gsalpha-dependent signaling pathways. *Proc. Natl. Acad. Sci. USA.* 105:16976–16981. http://dx.doi.org/10.1073/pnas.0802898105

Yao, D., Y. Huang, X. Huang, W. Wang, Q. Yan, L. Wei, W. Xin, S. Gerson, P. Stanley, J.B. Lowe, and L. Zhou. 2011. Protein O-fucosyltransferase 1 (Pofut1) regulates lymphoid and myeloid homeostasis through modulation of Notch receptor ligand interactions. *Blood.* 117:5652–5662. http://dx.doi.org/10.1182/blood-2010-12-326074

Zakrzewski, J.L., A.A. Kochman, S.X. Lu, T.H. Terwey, T.D. Kim, V.M. Hubbard, S.J. Muriglan, D. Suh, O.M. Smith, J. Grubin, et al. 2006. Adoptive transfer of T-cell precursors enhances T-cell reconstitution after allogeneic hematopoietic stem cell transplantation. *Nat. Med.* 12:1039–1047. http://dx.doi.org/10.1038/nm1463

Zhang, M., S. Xuan, M.L. Bouxsein, D. von Stechow, N. Akeno, M.C. Faugere, H. Malluche, G. Zhao, C.J. Rosen, A. Efstratiadis, and T.L. Clemens. 2002. Osteoblast-specific knockout of the insulin-like growth factor (IGF) receptor gene reveals an essential role of IGF signaling in bone matrix mineralization. *J. Biol. Chem.* 277:44005–44012. http://dx.doi.org/10.1074/jbc.M208265200

Zhu, J., R. Garrett, Y. Jung, Y. Zhang, N. Kim, J. Wang, G.J. Joe, E. Hexner, Y. Choi, R.S. Taichman, and S.G. Emerson. 2007. Osteoblasts support B-lymphocyte commitment and differentiation from hematopoietic stem cells. *Blood.* 109:3706–3712. http://dx.doi.org/10.1182/blood-2006-08-041384

Zlotoff, D.A., S.L. Zhang, M.E. De Obaldia, P.R. Hess, S.P. Todd, T.D. Logan, and A. Bhandoola. 2011. Delivery of progenitors to the thymus limits T-lineage reconstitution after bone marrow transplantation. *Blood.* 118:1962–1970. http://dx.doi.org/10.1182/blood-2010-12-324954